Jadeite Deposits of the Clear Creek Area, New Idria District, San Benito County, California[1]

U.S. Geological Survey, Menlo Park, California, U.S.A.

by R. G. COLEMAN

WITH ONE PLATE

ABSTRACT

Tectonic inclusions within the New Idria serpentine body contain jadeite in two distinct assemblages: (1) Lenslike inclusions containing a monomineralic green jadeite core surrounded by a calc-silicate rim. (2) Jadeite veins cross-cutting albite–crossite schist inclusions. In these veins jadeite coexists with low albite; green jadeite (Jd 75 Ac+Di+He 25) coexists with low albite within the host schist.

Albite schists are related to the pre-metamorphic keratophyres and it can be shown that desilication of such rocks produces a bulk composition similar to that of jadeite. Metamorphism of keratophyric tectonic inclusions within serpentine produced jadeite–albite schists along margins of the inclusions. Jadeite–albite veins formed from mobilized liquids rich in the jadeite molecule and deficient in water. Geological evidence such as would indicate extreme pressures or temperatures during jadeite formation is lacking; rather, a low silica and dry system allowed its formation at reduced temperatures and pressures.

INTRODUCTION

EXPERIMENTAL studies and reports on new occurrences of jadeite within the past ten years have brought this mineral from comparative obscurity to a place of importance in metamorphic petrology. It is the purpose of this paper to describe, in detail, the jadeite occurrence within the New Idria serpentine mass and, in the light of recent experimental evidence, to suggest a genesis.

Jadeite was first recorded in this area by Mielenz (1939) as small grains within quartz–albite–jadeite schist from localized metamorphic zones of the Franciscan formation of Jurassic and Cretaceous age which flanks the New Idria serpentine mass to the west. Within the serpentine mass, jadeite was originally identified by Dr. George Switzer, U.S. National Museum, in stream boulders collected by Bolander (1950) along Clear Creek. This discovery aroused considerable interest, as it was the first recorded occurrence of massive jadeite on the North American continent. Previously, the only known deposits of massive jadeite were those in Tawmaw, Upper Burma; Kotaki District, Niigata Prefecture, Japan; and Motagua Valley of Guatemala. Careful field-work by Yoder & Chesterman (1951) disclosed that the boulders found by Bolander were derived from outcrops along the slopes of Clear Creek. A preliminary mineralogical description was given by Coleman (1954, 1956) as part of a more comprehensive study of the New Idria serpentine mass (Coleman, 1957).

The massive jadeite from this locality forms in rocks distinct from the jadeitic

[1] Publication authorized by the Director, U.S. Geological Survey.

[Journal of Petrology, Vol. 2, Part 2, pp. 209–47, 1961]

metagraywackes described in recent papers by Bloxam (1956, 1959), De Roever (1955), McKee (1958), Seki & Shido (1959), and Shido & Seki (1959). These authors describe jadeitic pyroxene as an essential mineral in metagraywackes composed essentially of quartz–lawsonite–jadeitic pyroxene–glaucophane. Jadeite from Clear Creek occurs with a different mineral assemblage and is of different composition.

GENERAL GEOLOGY

The Clear Creek jadeite deposits are contained within an elongate serpentine dome about 12 miles long and 4 miles wide, situated within the New Idria District, California (Fig. 1). This District is located in the southern extension of the Diablo Range of the California Coast Ranges. The regional geology has been described by Eckel & Myers (1946), Anderson & Pack (1915), Mielenz (1939), Phillips (1939), and Jennings & Strand (1958). Their maps and discussions have been consulted, and in part incorporated into this description. A detailed map has been made of the serpentine mass (Coleman, 1957) and from this map the salient features related to this problem are taken and given in Fig. 2.

Structure. The serpentine mass lies between the San Andreas fault on the west and the Great Valley of California on the east. The sedimentary rocks in this area are folded into a series of anticlines and synclines trending N. 70° W., which is oblique to the N. 40° W. structural trend of the San Andreas fault (Jennings & Strand, 1958). The elongate oval body of serpentine is flanked by the Franciscan formation of Jurassic and Cretaceous age and the Panoche formation of Late Cretaceous age. These flanking sediments and the serpentine mass together comprise an asymmetric anticlinal dome that is the northern extension of the Coalinga anticline. Eckel & Myers (1946) have shown that the north-east flank of the dome is marked by overturned sediments that have assumed this attitude as a result of the irregular New Idria thrust fault which marks part of the serpentine-sediment contact. The remainder of the contact around the serpentine dome is marked by high-angle fault and shear zones. These structural relations suggest that the fault-bounded serpentine mass has moved upward through the Mesozoic sediments.

Serpentine body. The New Idria serpentine mass, as well as other serpentine bodies in the Franciscan formation of the California Coast Ranges, has been considered 'intrusive' into the Jurassic and Cretaceous sediments. Evidence to support intrusive emplacement is lacking. Faulted contacts and the non-existence of contact metamorphism imply that emplacement was effected by tectonic movement rather than by magmatic intrusion; therefore the age of the primary ultrabasic rock cannot be determined by the presently exposed contact relations. The original movement of the ultrabasic 'magma' into the earth's crust may well have been during the period of maximum down-warping of the Franciscan geosyncline. Tectonic movements following the original emplacement

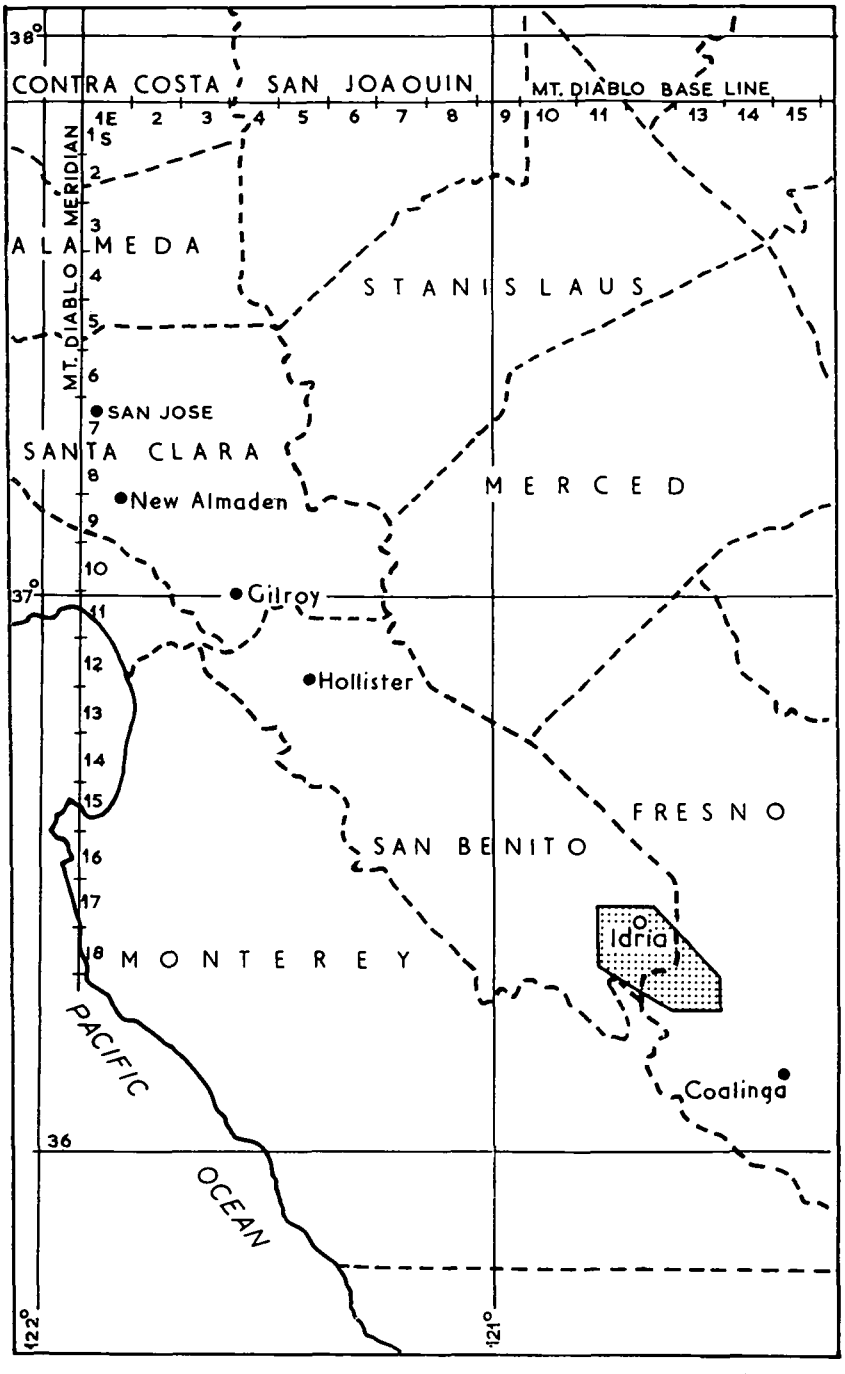

FIG. 1. Index map showing location of the New Idria District, California. After Eckel & Myers (1946).

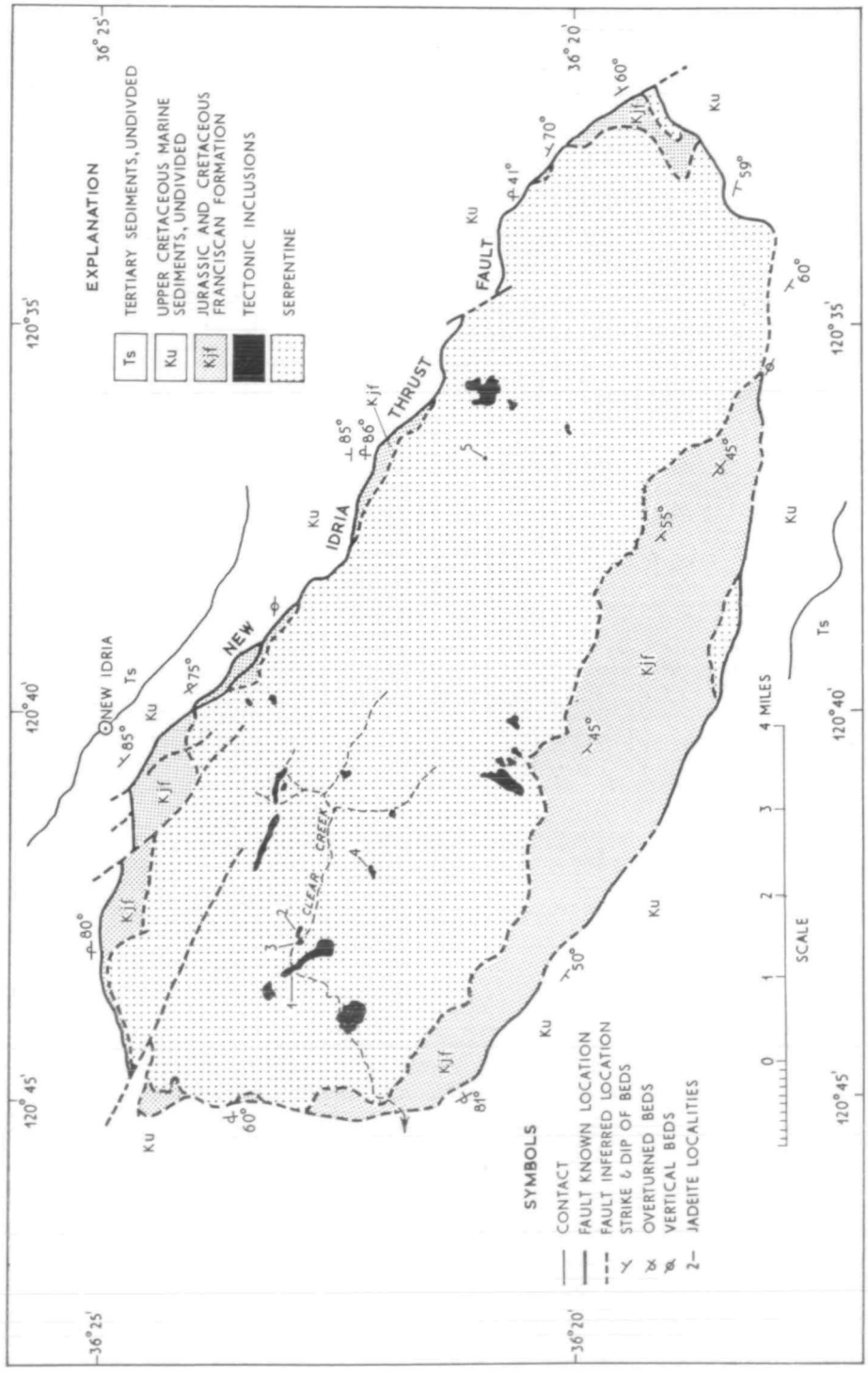

FIG. 2. Simplified geological map of the New Idria serpentine mass showing tectonic inclusions and jadeite localities. Modified from Eckel & Myers (1946).

of the ultrabasic rocks were probably instrumental in starting serpentinization and the squeezing of the mass into its present position. That emplacement of the serpentine was accomplished, undoubtedly, in several distinct stages is demonstrated by the presence of abundant serpentine debris in near-by sediments of three different ages (Eckel & Myers, 1946); Upper Cretaceous (Panoche formation), Upper Middle Miocene (Big Blue serpentinous member of the Temblor formation), and Pliocene (Tulare formation).

Tectonic inclusions. Jadeite-bearing rocks within the serpentine are found in tectonic inclusions. The distribution, size, and shape of the larger bodies are shown in Fig. 2. Smaller bodies associated with the larger masses, not shown on the map, may be less than 10 square feet in areal extent. Some of the larger bodies roughly parallel the regional NW.–SE. structural trend, but the smaller bodies are randomly orientated. Within each separate body the schistosity and planar structures are consistent; however, there is no correlation of these structures between each separate body. The inclusions were derived mainly from graywackes, tuffs, greenstones, spilites, keratophyres, and cherts characteristic of the Franciscan eugeosynclinal suite. In most cases, bedding and igneous textures have not been completely obscured by the attendant metamorphism of these inclusions.

Brothers (1954, p. 616) has described similar rock bodies within serpentines of the Berkeley Hills, California, and has referred to them as tectonic inclusions. Many other serpentine bodies within the California Coast Ranges contain foreign inclusions showing sheared contacts and random orientation. It is recommended that the term 'tectonic inclusions' be used to describe those inclusions, found within serpentines, which show random orientation and structural evidence of having been emplaced within the serpentine by tectonic movements—as originally set forth by Brothers.

The contacts between the serpentine and the inclusions are sheared and faulted; however, in some instances where macro-shearing or faulting are not apparent, microscopic examination reveals shearing and alteration of serpentine to chlorite and andradite. Careful examination of the contacts revealed no evidence of metamorphism, within the tectonic inclusions, that might have resulted from contact with an ultrabasic magma. There is some evidence of metasomatic interchange between the serpentine and inclusions. Sodium-rich pyroxenes are found to invade and replace the serpentine near the contacts and along the borders of smaller pod-like bodies, and introduction of calcium is demonstrated by the development of calc–silicate within the inclusions.

The movement of the tectonic inclusions within the New Idria serpentine mass is extremely difficult to interpret. The tabular and elongate shape of the inclusions, combined with the vertical dip of the bedding or schistosity, indicate vertical movement within the serpentine. Semi-parallel orientation of these inclusions with the bounding faults demonstrates that such an alignment may have developed during the upward squeezing of the semiplastic serpentine.

These relations suggest that the inclusions were incorporated into the ultrabasic rock during serpentinization, or after serpentinization as part of an intense tectonic movement within the Diablo Range.

Similarity of mineralogy and bulk composition of the tectonic inclusions to the Franciscan formation suggest that the inclusions are blocks of Franciscan emplaced within the serpentine. In no instance were tectonic inclusions found that could be definitely related to rocks younger than Franciscan, nor were there rocks present that could be classed as older basement rocks.

Low-grade metamorphism is characteristic of the tectonic inclusions and is similar to that of the glaucophane schists found within the Franciscan formation. However, the inclusions do not show complete recrystallization and they are uniformly finer grained than typical California glaucophane schist facies rocks. Evidence for retrogressive metamorphism, often described in the glaucophane schists of California, was not found in these inclusions.

Diverse rock types are represented within the inclusions but, as shown by Coleman (1957), their metamorphic grade is that of the glaucophane schist facies as defined by Fyfe, Turner, & Verhoogen (1958). Albite–crossite schists similar to those found within the inclusions are not widely developed within the glaucophane schists of the Franciscan formation; however, their presence has been established by Palache (1894), and Fyfe, Turner, & Verhoogen (1958). Edgar Bailey & Julius Schlocker, U.S. Geological Survey (oral communication, 1960), have also observed albite-blue amphibole schists within metamorphic terrains of the Franciscan formation in central and northern California. A small area of albite–glaucophane–chlorite schist outcrops within the Franciscan formation flanking the north-eastern part of the New Idria serpentine mass. Even though the albite-blue amphibole schists are not well known within the schist terrains of the Franciscan, and chemical analyses are not available to allow a precise comparison, it is evident that the albite–crossite schist tectonic inclusions are similar and can be correlated with albite-blue amphibole schists of similar bulk composition within the Franciscan formation. Jadeite is restricted to these quartz-free albite–crossite schist inclusions within the serpentine mass.

The relations between the albite–blueamphibole schists and the spilite–keratophyre lavas of the Franciscan will be treated in the section on petrology.

MINERALOGY

The mineralogy of the jadeite and the associated minerals is given in detail to characterize the deposits. For this purpose, representative rock types containing jadeite and associated minerals were carefully studied, rather than using the best development of a particular mineral. Mineral separations were made and each mineral identified by optical and X-ray techniques. Paragenetic relations were established from thin sections.

Jadeite. Jadeite from this area assumes varied habits and exhibits a rather wide range in composition. Nearly pure jadeite is found within veins cross-cutting

albite–crossite–acmite schists. Within these veins, jadeite is white with only a faint green tint developing along the vein contact. Earlier generations of green fibrous jadeite associated with albite are developed within the schists containing veins of white jadeite. Green jadeite also forms in pod-like bodies where it commonly exhibits cataclastic deformation and is healed by intersecting veins of white jadeite.

TABLE 1

Chemical analyses and optical properties of the Clear Creek Jd-rich pyroxenes, with atomic ratios

	1	2	3
SiO_2	59·38	59·06	56·54
Al_2O_3	25·82	24·62	18·38
TiO_2	0·04	0·08	0·44
Fe_2O_3	0·45	0·41	5·67
FeO	trace	0·18	1·05
MnO	nil	0·03	0·10
MgO	0·12	0·17	1·44
CaO	0·13	0·35	2·69
Na_2O	13·40	14·95	13·00
K_2O	0·02	0·01	0·03
H_2O^+	0·22	0·07	0·20
H_2O^-	0·16	0·03	0·05
Li_2O	—	nil	0·01
Cr_2O_3	0·01	—	—
TOTAL	99·75	99·96	99·60
S.G.	3·34±0·006	—	—
α	1·654	1·654	1·679
β	1·657	1·656	1·681
γ	1·666	1·666	1·685
Biref.	0·012	0·012	0·006
$2V_z$ (+)	70°±2°	70°±2°	64°±2°
$Z \wedge c$	34°±1°	35°±1°	38°±1°
Disp.	none	none	$r > v$ strong
Jd	96·5	97·6	74·3
Ac	2·4	1·0	15·1
Di	1·1	0·9	7·5
He	—	0·5	3·2

Metal atoms to 6 (O)

	1			2			3		
Si	1·999	1·999 Z		1·997	1·997 Z		1·981	2·000 Z	
Al	—			—			0·019		
Al	1·024			0·980			0·740		
Ti	0·011			0·002			0·011		
Fe^{3+}	0·011	1·042 X		0·010	1·006 X		0·146	1·004 X	
Fe^{2+}	—			0·005			0·030		
Mn	—		1·921	0·001		1·996	0·003		1·988
Mg	0·006			0·008			0·074		
Ca	0·005			0·012			0·101		
Na	0·873	0·879 Y		0·978	0·990 Y		0·882	0·984 Y	
K	0·001			—			0·001		

1. White jadeite from veins (54-RGC-58) in albite-green jadeite schist from tectonic inclusions (see Fig. 5), Clear Creek, New Idria District, California (Locality No. 2, Fig. 2). Analyst: W. H. Herdsman, Glasgow, Scotland. Na_2O value is apparently in error as calculation of the formula to 6 (O) reveals a large discrepancy between Z group and the Σ (XY) groups.
2. White jadeite (J31–14) Clear Creek, New Idria District, California (Locality No. 1, Fig. 2). Collected by H. S. Yoder jr. Analysed sample loaned to the author by G. S. Switzer, U.S. National Museum. Analyst: Eileen H. Oslund, Univ. of Minnesota.
3. Green jadeite (J28–7) Clear Creek, New Idria District, California (Locality No. 1, Fig. 2). Collected by H. S. Yoder jr. Analysed sample loaned to the author by G. S. Switzer, U.S. National Museum. Analyst: Eileen H. Oslund, Univ. of Minnesota.

X-ray and optical determinations were made on splits of the analysed samples.

Two analyses of the white-vein jadeite and one of the green jadeite are given in Table 1. White-vein jadeite is very nearly pure Jd ($NaAlSi_2O_6$) whereas the green jadeite contains some Ac ($NaFe^{3+}Si_2O_6$), Di ($CaMgSi_2O_6$), and He ($CaFe^{2+}Si_2O_6$). Calculations of these analyses to the components Jd, Ac, Di, and He were made following the system used by Hess (1949). A chemical comparison of the Clear Creek jadeite with other jadeites and related jadeitic pyroxenes is shown in Fig. 3. From this comparison it can be seen that many of the pyroxenes referred to as jadeite may contain considerable amounts of the

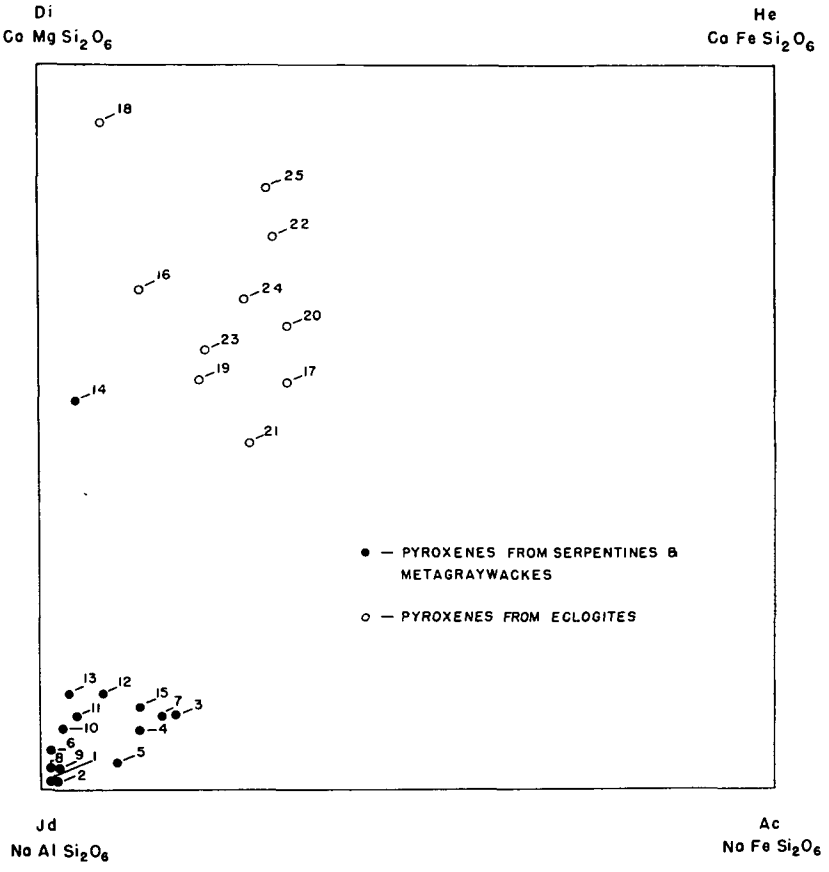

FIG. 3. Chemical variation of jadeitic pyroxenes represented by four components; Jd, Ac, Di, and He.

1, 2, 3. Clear Creek jadeites, see Table 1.

4. Jadeite from quartz–jadeite–lawsonite–glaucophane metagraywacke, 2½ miles N. 17° E. of Valley Ford, Sonoma County, California. Analysed material is impure; 12·55 per cent SiO_2 (quartz) was subtracted from the analysis before calculations were made. Analyst: Eileen H. Oslund, Univ. of Minnesota (Bloxam, 1956). (*Jd 80·0, Ac 11·2, Di 6·5, He 2·3.*)

5. Jadeite from quartz–jadeite–lawsonite–muscovite metagraywacke (blasto-psammitic quartzite) from Roesek River, between Korontowoe and Pompangeo Mountains 1° 48′ S., 120° 59′ W., Eastern Central Celebes. Analysed material impure; 5 per cent quartz, 0·44 per cent TiO_2 as rutile, and 0·15 per cent H_2O, subtracted by De Roever from analysis. Analyst: J. H. Scoon, Cambridge University (De Roever, 1955). (Jd 87·0, Ac 8·9, Di 2·7, He 1·5.)

6. Jadeite associated with quartz in veins cutting glaucophane schist. Boulders collected 2½ miles north of the Sonoma County–Mendocino County line in the bed of the Russian River, Cloverdale, California. Analysed material impure; 6 per cent quartz subtracted by Wolfe from analysis. Analyst: Eileen H. Oslund, Univ. of Minnesota (Wolfe, 1955). (Jd 93·1, Ac 0·9, Di 5·5, He 0·5.)

7. Jadeite from glaucophane schist, Valley Ford, Sonoma County, California. Supplied by Dr. George Switzer, U.S. National Museum. Analyst: Eileen H. Oslund, Univ. of Minnesota. (Jd 93·1, Ac 0·9, Di 5·5, He 0·5.)

8. Jadeite from Burma (U.S. N.M. No. 94829). It is assumed that this material came from the Tawmaw deposits within the serpentine mass. Analyst: E. G. Zies (Yoder, 1950*a*). (Jd 97·2, Ac 0·9, Di 1·9, He 0·0.)

9. White jadeite associated with albite in zoned pods surrounded by serpentine from Kotaki District, Niigata Prefecture, Japan. Recalculation of the analysis to fit the pyroxene formula shows the Na_2O determination is in error as in No. 1. Data taken from Yoder (1950*a*) as derived from Omori (*1939*) and Kawano (*1939*). (Jd 94·7, Ac 2·1, Di 3·2, He 0·0.)

10. Green jadeite associated with albite in zoned pods surrounded by serpentine from Kotaki District, Niigata Prefecture, Japan. Comments identical with those above. (Jd 89·2, Ac 2·3, Di 8·0, He 0·5.)

11–15. 'Blue Jade', Mexico. (Jd 86·4, Ac 3·2, Di 8·7, He 0·7.) 12. Jadeite from large pea-green coloured celt, Guatemala. (Jd 80·4, Ac 6·4, Di 11·7, He 1·5.) 13. Jadeite from boulder (No. 2078) tomb, Kaminaljuyu, Guatemala. (Jd 84·5, Ac 1·9, Di 11·9, He 1·7.) 14. Diopside–jadeite rough fragment, Kaminaljuyu, Guatemala. (Jd 44·6, Ac 2·4, Di 50·8, He 2·2.) 15. Chloromelanite from greyish-green celt, Guatemala. (Jd 76·0, Ac 12·2, Di 10·4, He 1·5.) These Meso-American jadeites are associated with low albite and, to a lesser extent, muscovite, sphene, actinolite, and zoisite. Although they have not been found in place, Foshag (1955) suggests that these gemstones form in and near the serpentine bodies of Guatemala. Analyst: Joseph Fahey, U.S. Geological Survey (Foshag 1955, 1957).

16–18. Omphacite in eclogite (omphacite 57 per cent, garnet 34 per cent, quartz-mica 7·9 per cent) from Silden, Nord-

other pyroxene components. For instance, green jadeite (Table 1, No. 3) from Clear Creek contains 25·9 per cent of other pyroxene components, yet it is clearly much closer to pure jadeite composition than much other 'jadeite'. Substitution of other components into pure jadeite produces an increase in the indices and extinction angle, but lowers the density, birefringence, and optic angle. It is not possible at this time, to correlate these changes in optical properties with variation of Ac, Di, and He components within jadeitic pyroxenes. A characteristic of the jadeitic pyroxenes containing between 10 and 30 per cent Di, He, and Ac, however, is worthy of special comment (see especially Nos. 3, 4, 5, and 7, Fig. 3). These pyroxenes have a very strong dispersion ($r > v$) combined with a low birefringence (0·006–0·008) in this compositional range. These properties have been previously observed by Bloxam (1956) and De Roever (1955) for jadeitic pyroxenes within metagraywackes and Shido & Seki (1959) report the same optical character for jadeitic pyroxenes in metamorphosed mafic intrusives. The strong dispersion and low birefringence in jadeitic pyroxenes of this composition may cause serious errors in identification, as clinozoisite could easily be confused with jadeite when the determination is based on a thin-section study.

In Table 2, X-ray diffraction patterns of the analysed jadeites from Clear Creek are compared with jadeitic pyroxene from metagraywacke, and the data given by Yoder (1950*a*) for an analysed Burmese jadeite. The Clear Creek white-vein jadeite closely matches the spacings given for the Burma material; however, the jadeitic pyroxenes rich in Ac, Di, and He components show noteworthy changes in the (330), (441), (310), and (311) spacings. In addition to the shift in *d*-spacings, a weak but persistent peak at 21·0 Å is characteristic for the Ac–Di–He-rich jadeites (Table 2). This peak at 21·0 Å (001?) indicates the possibility of a super cell for jadeites of this composition and having a *c*-dimension exactly four times that given for pure jadeite. These changes reflect an increase in the *a* and *b* cell dimensions as it has been shown by Yoder (1950*a*), Wolfe (1955), Schüller (1958), and Warren & Biscoe (1931), that the *c*-dimension for all pyroxenes is essentially constant. Again, it is apparent that substitution of Di,

---

fjord, Norway. Analyst: P. Eskola. (Jd 22·2, Ac 8·1, Di 64·3, He 6·5.) 17. Omphacite in Duen type eclogite (omphacite 38 per cent, garnet 55 per cent, apatite 5 per cent), Norway. Analyst: L. Thomasen. (Jd 36·4, Ac 16·8, Di 30·0, He 16·8.) 18. Omphacite in eclogite (omphacite 55 per cent, garnet 44·8 per cent) from Rodhaugen, Almklovdalen, Sondmore, Norway. Analyst: P. Eskola. (Jd 3·3, Ac 4·5, Di 88·0, He 4·2.) These are typical omphacites from eclogites (Eskola, 1921).

19. Omphacite in eclogite (omphacite 57 per cent, garnet 28 per cent, glaucophane 2 per cent, hornblende 3 per cent, chloride 4 per cent, sphene 4 per cent, and rutile 2 per cent) from Healdsburg, Sonoma County, California. Analyst: F. A. Gonyer (Switzer, 1945). (Jd 31·4, Ac 11·6, Di 46·9, He 10·1.)

20. Omphacite in eclogite (omphacite and garnet) from Ardintoul, Glenelg, Scotland. Analyst: A. R. Alderman (Alderman, 1936). (Jd 31·5, Ac 11·5, Di 46·9, He 10·1.)

21. Omphacite in eclogite (omphacite, garnet, rutile, and apatite) from Fay, France. Analyst: Raoult (Briere, 1920). (Jd 35·0, Ac 16·9, Di 36·8, He 11·3.)

22. Omphacite in a garnet–hornblende–pyroxene–scapolite gneiss from Ghana, Africa. Pyroxene from this rock is considered transitional between the amphibolite and eclogite facies. Analyst: O. von Knorring (von Knorring & Kennedy, 1958). (Jd 1·8, Ac 11·2, Di 66·0, He 21·0.)

23. Omphacite in eclogite (omphacite and garnet) from Valley Ford, Sonoma County, California. This eclogite is in close association with the jadeite-bearing metagraywackes of this area. Analyst: T. W. Bloxam (Bloxam, 1959). (Jd 32·0, Ac 6·9, Di 45·9, He 15·2.)

24. Omphacite in eclogite (omphacite and garnet), hills west of 'Postman's Path' to Ardintoul, Glenelg, Scotland. Analyst: J. H. Scoon, Cambridge University (Yoder & Tilley, 1959). (Jd 18·7, Ac 13·2, Di 53·3, He 14·8.)

25. Omphacite in eclogite (omphacite and garnet), ¼ mile south-east of the Pier, Totaig, Loch Duich, Ross-shire (Yoder & Tilley, 1959). (Jd 6·1, Ac 10·7, Di 63·0, He 20·3.)

TABLE 2

*X-ray powder diffraction data on Jd-rich pyroxenes**

Space Group C_{2h}^6 *hkl*	1		8		3		B-48	
	d	*I*	*d*	*I*	*d*	*I*	*d*	*I*
	(Å)		(Å)		(Å)		(Å)	
?	—	—	—	—	21·0	½	21·0	½
110	6·20	2	6·18	1	6·27	2	6·20	2
200	4·50	½	4·49	½	N.O.	—	W.B.	—
020	4·29	4	4·27	3	4·34	2	4·29	3
021	3·25	½	3·25	1	3·26	½	3·25	½
220	3·10	3	3·10	3	3·13	2	3·11	2
221	2·92	7	2·92	8	2·94	6	2·93	5
310, 311	2·83	10	2·83	10	2·85	10	2·84	10
130	N.O.	—	2·68	½	N.O.	—	N.O.	—
202, 002, 131, 112	2·49	4	2·49	2	2·50	2	2·49	2
$\bar{2}21$	2·42	5	2·42	9	2·44	2	2·42	3
$13\bar{1}$	N.O.	—	2·31	½	N.O.	—	N.O.	—
400	N.O.	—	2·24	½	N.O.	—	N.O.	—
312	2·21	1	2·20	2	2·22	1	2·21	1½
022	2·16	½	2·15	1	2·18	1	2·17	½
330	2·067	6	2·067	3	2·081	2	2·073	2
421	2·045	½	2·043	1	2·062	½	2·054	1
420	1·993	½	1·991	½	N.O.	—	1·997	½
041	1·969	4	1·966	1	1·982	½	1·973	1
241	1·888	½	1·887	1	1·914	½	1·892	½
511	1·831	½	1·835	½	N.O.	—	1·842	½
510	1·762	1	1·760	2	1·772	1	1·765	1
422	1·810	½	1·807	½	1·822	½	1·820	½
332	1·683	½	1·683	2	1·698	½	1·689	1
042	1·623	½	1·623	½	1·642	½	1·629	½
313	1·653	½	1·652	½	1·675	½	1·656	½
441	1·573	3	1·570	4	1·583	½	1·577	1
223	1·610	½	1·608	½	1·615	½	1·613	½
440	1·550	2	1·551	1	1·559	½	1·556	½
530	1·523	½	1·523	½	N.O.	—	1·528	½
600	1·499	1	1·498	1	1·502	½	1·504	½
350	1·487	1	1·488	1	W.B.	—	1·497	½

* X-ray patterns were obtained with a Norelco high-angle diffractometer using Cu K_α radiation. *d*-spacings between 3° and 62° 2θ are recorded. $I = I_{hkl}/I_{10}$; N.O. = not observed; W.B. = weak and broad peak.

1. White jadeite (54-RGC-58) from vein. Analysed, Table 1, No. 1 (Jd 96·5, Ac 2·4, Di 1·1).
8. Jadeite from Burma (U.S. N.M. No. 94829). Analysed (Jd 95·8, Ac 0·9, Di 2·9). X-ray data taken from Yoder (1950*a*).
3. Green jadeite (J28-7). Collected by H. S. Yoder jr. Analysed, Table 1, No. 3 (Jd 74·3, Ac 15·1, Di 7·6, He 3·2).
B-48. Jd-rich pyroxene from quartz–jadeite–lawsonite–sericite schist (metagraywacke), Angel Island, San Francisco Bay, California. Analysis of this jadeite pending.

Ac, and He components produce marked changes in the properties of jadeite; however, as shown earlier, it is not possible to determine the effect of each individual component.

Further observations can be made from Fig. 3 that apply directly to the Clear Creek deposits and their relations to other jadeitic pyroxenes described in the literature. From the figure, it is readily apparent that jadeites from serpentines and metagraywackes form a distinct group containing less than 30 molecular per cent of Di, He, and Ac, whereas pyroxenes from eclogites, containing as much as 64 molecular per cent Jd, have a much wider range of solid solution but do not overlap the jadeites. This difference in the two types of pyroxene was defined earlier by Yoder (1950*a*) on the basis of geological association. The present study demonstrates that the pyroxenes from the Clear Creek deposits are clearly different from the omphacites reported from eclogites.

In the discussion to follow, the use of the term '*white* jadeite' will be used to designate pyroxene with at least 95 molecular per cent Jd and '*green* jadeite' will be used to describe pyroxene containing 5–30 molecular per cent of combined Di, Ac, and He. Optical and X-ray studies of various types of green jadeite, both in the pods and in albite–jadeite schists, demonstrate that their composition is similar to the analysed green jadeite (Table 1, No. 3).

Within the albite–crossite schists, small porphyroblasts of a green pyroxene are commonly developed along iron-rich stringers of the schists. Insufficient material was available for analyses, but the determined optical properties are similar to those of acmite: $\alpha = 1{\cdot}740 \pm 0{\cdot}002$; $2V_x = 75$–$80°$ (−), $X \wedge c = 16°$, X = light green, Y = colourless, Z = light yellow. Similar pyroxenes (Ac 48±, Jd 7±, Di 45±) are reported from albite–aegirine–augite and aegirine–augite–blue amphibole–garnet–albite–quartz schists from Sikoku, Japan (Banno, 1959).

Albite. Plagioclase is a common associate of jadeite formed within the schistose tectonic inclusions, but within the pod-like jadeite deposits albite is not present. The following discussion, therefore, will refer only to albite coexisting with jadeite in veins or as a major constituent of the schist making up the tectonic inclusions.

Coarsely crystalline, vein albite develops as radiating clusters intergrown with, or partially replacing, jadeite. Later veins of albite cut the jadeite veins and within these late veins albite is intergrown with pectolite and thomsonite. Simple albite twinning is observed in some grains, but many individuals do not exhibit twinning. Within the tectonic inclusions, albite may make up as much as 50 per cent of the schists. Here the albite is extremely fine-grained and untwinned; however, the larger porphyroblasts of albite within the groundmass are characterized by simple albite twinning.

To establish the composition of the albite it was separated from the veins and schists by carefully controlling a bromoform–acetone mixture between a density of 2·64 and 2·65, and centrifuging. This density suggested a compositional range near that of pure albite, which was confirmed by a spectrographic analysis of the

vein feldspar (0·1–0·5 per cent Ca, and less than 0·3 per cent K). The structural state was established by the X-ray diffraction technique described by J. V. Smith (1956) and J. R. Smith & Yoder (1956).

TABLE 3

Composition of the plagioclase determined by the separations ($\bar{1}32$–131), (131–$1\bar{3}1$), *and* (111–$1\bar{1}1$) *after J. V. Smith* (1956)

	$\bar{1}32$–131	% An	131–$1\bar{3}1$	% An	111–$1\bar{1}1$	% An
54-RGC-58 Albite from jadeite veins; analysed jadeite from same specimen	2·725	2·0	1·051	0·0	0·48	2·0
54-RGC-58-1 Albite from albite–crossite schist*	2·72	3·0	1·10	2·0	0·47	1·0
54-RGC-58-2 Albite from albite–crossite–stilpnomelane schist	2·725	2·0	1·053	0·0	0·48	2·0
54-RGC-58-3 Albite from albite–crossite–acmite schist	2·735	1·3	1·10	2·0	0·46	0·0
54-RGC-58-4 Albite from albite–crossite schist	2·73	2·0	1·095	2·0	0·48	2·0
54-RGC-58-5 Albite from albite–crossite–acmite schist	2·705	3·0	1·062	0·0	0·46	0·0
54-RGC-58-6 Albite from albite–crossite schist (analysed rock, see Table 8, No. 3)	2·715	3·0	1·09	1·8	0·48	2·0
54-RGC-58-7 Albite from albite–crossite schist	2·71	2·6	1·043	0·0	0·45	0·0
54-RGC-58-8 Albite from albite–crossite–acmite schist	2·72	3·0	1·07	0·4	0·47	1·0
54-RGC-58-9 Albite from albite–crossite–acmite schist	2·72	3·0	1·08	1·0	0·45	0·0

* Schist samples represent a series of samples taken across the tectonic inclusion shown in Fig. 4.

The separation 2θ ($\bar{1}32$)–2θ (131) on all samples ranged between 2·705 and 2·735 (Table 3). From fig. 4 of J. V. Smith's paper, these values all fall close to the low-temperature curve at Ab_{100} composition. Measurements of the separation 2θ (131)–2θ ($1\bar{3}1$) gave values ranging from 1·05 to 1·10, which, from fig. 3 of Smith, correspond to compositions lying between An_0 and An_2 (Table 3). Thus, as suggested by Smith, the separations 2θ ($\bar{1}32$)–2θ (131) and 2θ (111)–2θ ($1\bar{1}1$) can be used to establish the composition of low albites, as has been done in Table 3.

It has been pointed out by J. R. Smith & Yoder (1956), J. V. Smith (1956), and MacKenzie (1957) that the values so determined are only reliable within ± 2 per cent An and that curves constructed from synthetic and natural feldspars may be valid only for those plagioclases used to establish them. However, the composition and structural state of the albite associated with the jadeite is now as well known as it conveniently can be, namely, between An_0 and An_2 and of the low form.

Zeolites. The presence of zeolites was established in all the tectonic inclusions bearing jadeite; however, some zeolites were restricted in their distribution.

Identification was based on optical and X-ray powder patterns of separated fractions obtained from the various rock types.

Thomsonite is present within the jadeite vein systems of the tectonic inclusions and also within the calc–silicate zone surrounding the pod-like jadeite bodies. It occurs as equigranular aggregates rarely exhibiting euhedral forms. Natrolite and pectolite occur as inclusions or are intergrown with the thomsonite. X-ray diffraction and optical data for thomsonite from the calc–silicate zone surrounding the jadeite pods are given in Table 4. Following Hey's (1932) data for thomsonite, this material must have a composition near that of the calcium-rich types.

TABLE 4

*X-ray diffraction and optical data for thomsonite**

d (Å)	*I*	*d* (Å)	*I*	*d* (Å)	*I*	*Optics*
6·55	50	3·52	60	2·69	60	$\alpha = 1{\cdot}528 \pm 0{\cdot}002$
5·94	10	3·29	15	2·585	20	$\beta = 1{\cdot}529 \pm 0{\cdot}002$
5·40	10	3·22	15	2·437	10	$\gamma = 1{\cdot}541 \pm 0{\cdot}002$
4·65	100	3·19	15	2·259	30	$2V(+) = 50°$ *ca*
4·39	15	2·96	20	2·197	60	
4·15	50	2·93	20	2·181	60	

Cu K_α radiation; $I = I_{hkl}/I_{100}$; *d*-spacings given for first 18 lines.

* *Thomsonite associated with pectolite and hydrogarnet in veins cutting calc-silicate zone, jadeite pods (105-RGC-58), shown in Fig. 6.*

Natrolite tends to crystallize as equigranular masses similar to thomsonite. However, within the jadeite vein system of the tectonic inclusions, it may be seen as large radiating groups intergrown with pectolite. It is most abundant within the veins and is of only minor importance in the calc–silicate zone of the jadeite pods. The following optical constants were obtained on the natrolite from veins cutting schist: $\alpha = 1{\cdot}476 \pm 0{\cdot}002$, $\beta = 1{\cdot}478 \pm 0{\cdot}002$, $\gamma = 1{\cdot}488 \pm 0{\cdot}002$, $2V(+) = 56° \pm 2°$.

Analcime is the least abundant zeolite and is generally restricted to veins within the tectonic schist inclusions. It replaces jadeite and/or albite as irregular wormy patches. Recent work by Saha (1959) on natural and synthetic analcimes allows us to estimate its composition by use of refractive index and unit cell measurements. For the Clear Creek analcime, a unit cell of 13·74 Å and a mean index of refraction of $1{\cdot}488 \pm 0{\cdot}003$ were recorded. Using figs. 1 and 3 of Saha (op. cit., pp. 303, 304) the molecular ratio of SiO_2 was found to be 4, and from this we can say that the composition of this analcime is very near the ideal, i.e $NaAlSi_2O_6 . H_2O$.

Hydrogrossular. Within the calc–silicate zone surrounding the jadeite pods, hydrogrossular forms as irregular masses intergrown with pectolite and thomsonite. Late veins of thomsonite–pectolite invading the calc–silicate rim contain irregular blebs of hydrogrossular closely associated with pectolite. Individual grains within these veins exhibit distinct zoning manifested by differences in

refractive index; the indices increase from the core outward. Hydrogrossular was not identified in the veins cutting the tectonic inclusions.

To establish the compositional range of the hydrogrossular in the calc-silicate zone and in the later veins cutting it, −300 mesh material was centrifuged in liquids of known densities to produce a series of fractions. The resultant density fractions, although contaminated with pectolite, were used to establish the refractive index and unit cell constants of the hydrogrossular (Table 5). It should be noted that the refractive indices suggest a wider range in composition than do the unit cell determinations, as the X-ray values represent an average

TABLE 5

*Physical constants for hydrogarnets and the composition determined from the refractive index, density, and unit cell size**

Garnet from	*Refractive index*	*Density*	*Unit cell in Å*	*Composition range*
Thomsonite–pectolite veins	1·643–1·700	2·92–3·31	11·98–12·15	$1{\cdot}5H_2O$ to $3H_2O$
Calc–silicate zone	1·67 –1·691	3·00–3·25	12·05–12·09	$2H_2O$ to $2{\cdot}5H_2O$

* Samples taken from pod-like body shown in Fig. 6.

value, whereas the lowest and highest indices are given. Using the data of Hutton (1943, p. 174), Yoder (1950*b*, p. 243), Flint *et al.* (1941), and Carlson (1956) on the grossularite–isometric tricalcium alumina hexyhydrate solid-solution series, the compositional range of the two occurrences was estimated.

To check the validity of the estimated hydrogrossular compositions, a fraction nearly free from pectolite was used by the author for a quantitative water determination. Total water was calculated as loss of weight after being heated in a platinum crucible at 900° C for 2 h in a muffle furnace. This fraction has an average refractive index of $1{\cdot}675\pm0{\cdot}005$ and a unit cell edge of $12{\cdot}06\pm0{\cdot}01$ Å, which correspond to hydrogrossular containing 2·40 moles of H_2O. The water determination gave 12·40 per cent H_2O, equivalent to 2·48 moles of H_2O in the hydrogarnet formula. Assuming, then, that the values so obtained are an estimate of the hydrogrossular composition in the series $3CaO.Al_2O_3.3SiO_2$—$3CaO.Al_2O_3.6H_2O$, the hydrogrossulars within the calc-silicate zone range in composition from $3CaO.Al_2O_3.1{\cdot}5SiO_2.3H_2O$ to $3CaO.Al_2O_3.2{\cdot}25SiO_2.1{\cdot}5$ H_2O.

Using the nomenclature of Hutton (1943), these would fall in the hydrogrossular series which includes 'hibschite' (Pabst, 1942), 'plazolite' (Foshag, 1920), and 'grossularoid' (Belyankin & Petrov, 1941). According to Hutton, no natural minerals in this series more hydrous than 'plazolite' have been found. The Clear Creek material, therefore, appears to be the first recorded hydrogrossular to contain nearly 14 per cent H_2O.

Pectolite. Considerable difficulty was experienced in establishing the identity of pectolite within the Clear Creek rocks. The fibrous and fine-grained nature of

this material makes it difficult to handle by optical techniques and originally it was reported as prehnite (Coleman, 1954). The refractive indices and density are nearly identical for pectolite and iron-free prehnite, and as pectolite is elongated on the *b*-axis ($Z \wedge b = 1$–$2°$) it can easily be mistaken as having the orthorhombic symmetry of prehnite. Furthermore, the strongest lines of X-ray patterns for these two minerals coincide, particularly those at 3·08 Å. X-ray powder patterns

TABLE 6

Analyses and optical data for pectolites

	1	2	3	*Atomic ratios for No. 1*		
SiO_2	53·84	54·23	52·99	Si	2·993	3·00
Al_2O_3	0·16	—	—	Al	0·010	
FeO	0·07	—	0·15	Fe	0·003	2·02
MgO	0·09	—	—	Mn	0·002	
CaO	33·74	33·74	32·98	Mg	0·006	
Na_2O	8·82	9·32	8·97	Ca	2·010	
MnO	0·04	—	—	Na	0·951	0·95
K_2O	0·019	—	—	K	—	
H_2O^+	2·96	2·71	3·30	OH	1·097	1·10
SrO	0·002	—	—			
CuO	0·004	—	—			
Others	—	—	0·56			
TOTAL	99·75	100·00	98·95			
H_2O^-	0·10	—	—			
S.G.	2·86±0·005	2·86	2·86			
α	1·598±0·003	1·595	1·595			
β	1·606 (calc.)	1·605	1·604			
γ	1·623	1·633	1·632			
Biref.	0·026	0·038	0·037			
$2V(+)$	35°±5°	63°	60°			

1. Pectolite (6-RGC-58) from tectonic inclusion in serpentine, Myrtle Creek, Oregon. Analytical separates by Sarah T. Neil; spectrographic analysis of separates: Raymond G. Havens and Arthur A. Chodos; calculations by Rollin E. Stevens and Sarah T. Neil.
2. Theoretical pectolite from Schaller (1955).
3. Pectolite from Japan, by Harada, as taken from Schaller (1955); 0·56 per cent listed as 'others' was not specified.

of this material, obtained at a later time, were found to match very closely prehnite patterns available to the author. Unfortunately, published X-ray powder patterns of pectolite exhibited many variations in intensity or spacings and did not appear to match the Clear Creek material, and it was not until an analysis was made that the identity of the Clear Creek pectolite was established.

An excellent sample of pectolite from a tectonic inclusion within a serpentine body near Myrtle Creek, Oregon, was purified and chemically analysed (Table 6). Its composition is identical with the manganese and iron-free pectolites described by Schaller (1955); however, the gamma index, $2V$, and birefringence of the Oregon material are lower than the values given by Schaller (1955). The X-ray powder data agree fairly well with those given by Schaller (1955) and Hildebrand (1953) except that the intensities are not comparable. These differences could be explained by preferred orientation—a common problem with

fibrous minerals, as shown by Hildebrand. Comparison of the X-ray data for the Oregon pectolite and the Clear Creek material demonstrates their similarity (Table 7). Optical determinations are identical with all samples showing the anomalously low gamma index (1·623), birefringence, and $2V$. No apparent explanation can be found for the optical discrepancies between these pectolites and those described in the literature.

TABLE 7

X-ray diffraction data for pectolite

1		2		3		4	
d	*I*	*d*	*I*	*d*	*I*	*d*	*I*
7·76	10	7·76	5	7·80	10	7·83	5
6·98	10	7·14	10	7·03	10	7·03	5
5·45	10	5·45	5	5·47	10	5·50	5
3·88	50	3·88	30	3·88	40	3·90	6
3·50	40	3·50	50	3·50	50	3·52	5
3·30	70	3·30	60	3·31	60	3·33	6 B
3·26	80	3·26	75	3·27	60	3·28	
3·08	100	3·08	100	3·08	100	3·10	8
2·90	50	2·90	80	2·91	50	2·921	10
2·73	40	2·72	60	2·73	30	2·729	6
2·59	50	2·59	50	2·59	40	2·600	6
2·417	5	Not observed		Not observed		2·430	5
2·327	10	2·339	10	2·334	10	2·338	5
2·292	40	2·292	20	2·295	30	2·298	6
Not observed		Not observed		Not observed		2·227	2
2·181	10	2·176	5	2·184	10	2·191	6 B
2·161	10	Not observed		2·166	5	2·166	

1. Analysed pectolite (6-RGC-58) from tectonic inclusion in serpentine, Myrtle Creek, Oregon.
2. Pectolite (104-RGC-58 (2)) from calc-silicate zone surrounding jadeite pods (Fig. 6).
3. Pectolite (104-RGC-58 (4)) from late veins in calc-silicate zone surrounding jadeite pods (Fig. 6).
4. Pectolite from Bergen Hill, New Jersey. U.S. N.M. 82952, Schaller (1955).

Cu K_α radiation diffractometer; $I = I_{hkl}/I_{100}$; partial patterns, B-broad.

Identification of the hydrated calcium aluminum silicates such as pectolite and prehnite is difficult in fine-grained metamorphic rocks and it is suggested that such determinations be based on careful optical and X-ray determinations.

Other minerals. Within the jadeite-bearing rocks and the associated schists are various minerals whose optical and other properties are listed below.

A fibrous blue amphibole within the schist bodies forms delicate needles, aggregates of fibrous bundles, or 'whisker-like' mattes. The optical character is similar to that given for crossite: $\beta = 1{\cdot}662 \pm 0{\cdot}002$, $Y \wedge c = 30$–$40°$, $2V = 10$–$20°$ (−), X = yellow, Y = greenish blue, Z = deep blue.

Red-brown stilpnomelane is a common associate of the blue amphibole within the albite–crossite schists. Using Hutton's (1956) data for the stilpnomelane group, the optical character of the Clear Creek stilpnomelane indicates a $(Fe^{2+}, Mn, Mg)\,0 : (Al, Fe^{3+})_2O_3$ ratio of about 1:1 ($\gamma = 1{\cdot}69 \pm 0{\cdot}005$, $2V = 0°$ (−), X = dark greenish brown, $Y = Z$ = light yellow-brown).

The chlorite associated with the thomsonite–pectolite–hydrogrossular in the

calc–silicate zone of the jadeite pods has the following optical properties: $\beta = 1{\cdot}59 \pm 0{\cdot}005$, $2V = 5$–$10°$ (−) X = light yellowish brown, $Y = Z$ = dark brown, birefringence moderate.

Carbonates are present both in the albite–crossite schists and in the calc–silicate zone of the jadeite pods. The density range for most of these carbonates was found to be between 2·90 and 3·00. The optics are $\alpha = 1{\cdot}530$, $\gamma = 1{\cdot}685$, $2V$ = approx. 20° (−), and the X-ray pattern match the standard for aragonite. On the basis of this data, the carbonate associated with the Clear Creek jadeite deposits is tentatively called aragonite.

Green biotite from veinlets within the jadeite pods has the following optics: $\beta = 1{\cdot}64$, $2V$ = small (−). This is the only mica found in these deposits.

Native copper is present as small isolated blebs (less than 1 mm) within the jadeite pods; the total amount is not significant enough to warrant more than a mention of its presence.

PETROLOGY OF THE JADEITE-BEARING ROCKS

Those rock types genetically associated with the jadeite deposits will be described in detail. The fine-grained nature of these rocks precludes any statements on the modal composition. Two distinct environments have been recognized for the jadeite deposits: (1) tectonic inclusions of schist containing jadeite as an essential mineral or in cross-cutting veins, and (2) pod-like bodies characterized by a central core of jadeite surrounded by a calc–silicate rim. In the discussion to follow, these two types will be treated separately.

Tectonic inclusions. As shown earlier, the tectonic inclusions within the serpentine mass have lithologies that are similar to the units that make up the Franciscan formation. Jadeite develops only within particular types that are high in albite and contain no free quartz. The typical greenstones and graywackes present within the serpentine mass as tectonic inclusions do not contain jadeite.

A detailed sketch-map of one of these jadeite-bearing inclusions is shown in Fig. 4. This body is composed of a very fine-grained banded schist. Slaty cleavage developed parallel to the original bedding, and cross-joints normal to the bedding, contain jadeite–albite grading into albite–zeolite minerals. The banded schist is light grey-green to dark bluish green according to the minerals developed along the original bedding planes.

Under the microscope, these rocks are fine-grained (0·1–0·5 mm grain size) with the largest individual grains rarely exceeding 0·3 mm. Albite, the most abundant mineral, forms an equigranular mosaic groundmass. Polysynthetic twinning is rarely developed in the groundmass feldspar; however, larger porphyroblastic grains commonly exhibit simple albite twinning. Crossite is the dominant dark mineral (5 to 25 per cent of the schist) forming delicate needles along shear planes, aggregates of fibrous bundles, or 'whisker-like' mattes.

Acmitic pyroxene, ubiquitous in these schists, makes up to 5 per cent of some

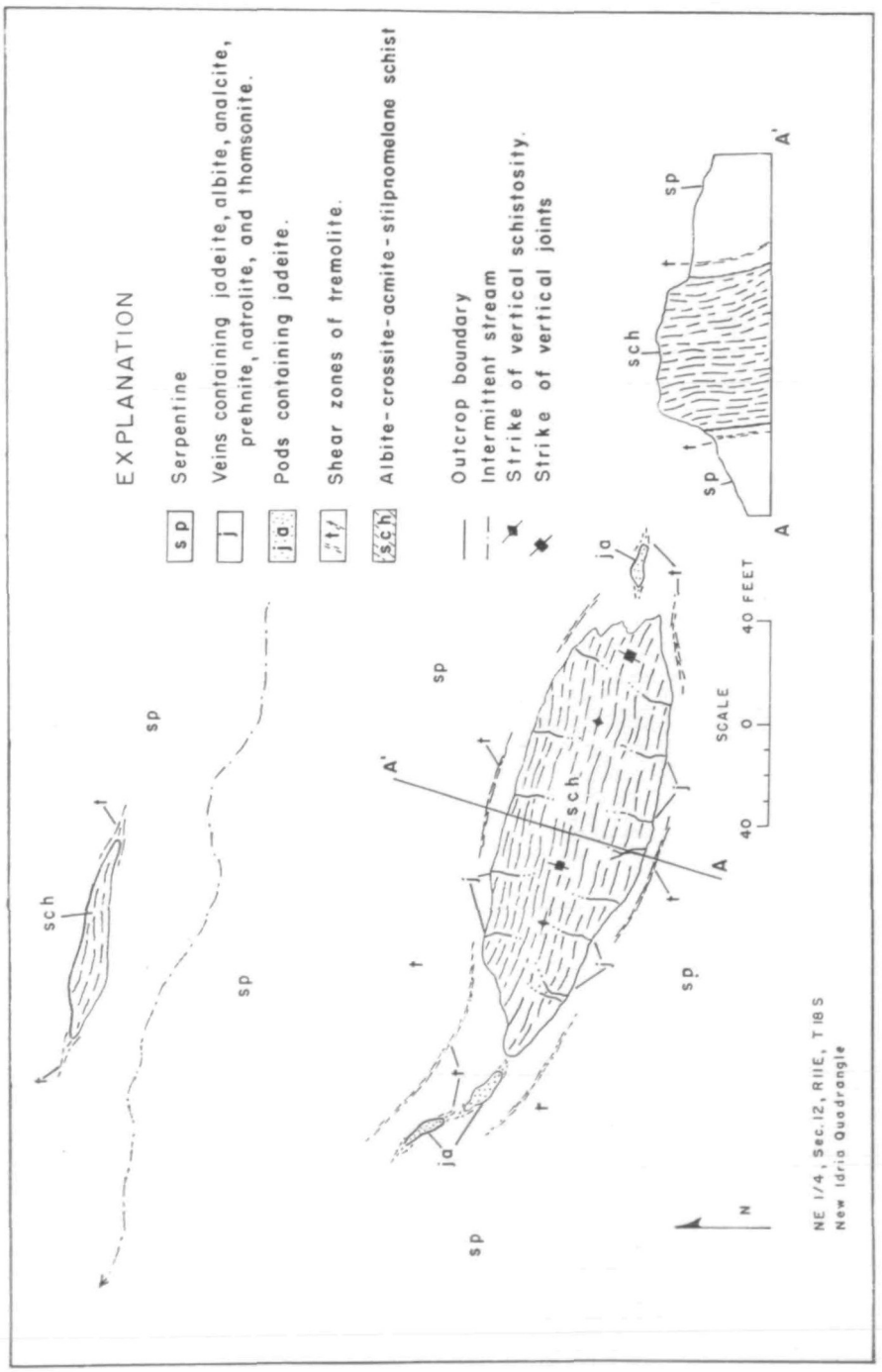

FIG. 4. Geological sketch-map of jadeite-bearing tectonic inclusion, Locality No. 2 shown in Fig. 2 (54-RGC-58).

of the darker-coloured schists. Its formation is favoured along shear planes containing abundant opaque material, and many grains characteristically contain relict opaque grains in their core. Sphene, pleochroic from pink to colourless, commonly forms in the opaque shear planes with the acmite. Stilpnomelane is a common accessory mineral of these schists, but rarely exceeds 1 or 2 per cent of the rock. Zircon was recognized in all the heavy residues (S.G. $> 2{\cdot}86$) of these schists.

Opaque material is concentrated along shear planes, forming crude segregation bands, and here blue amphibole, sphene, stilpnomelane, and acmite become concentrated. These opaque bands probably contained iron and titanium oxides that gave rise to the iron-rich silicates. Quartz was not found in any of the albite–crossite–stilpnomelane–acmite schists.

Folia paralleling the schistosity, within the lighter-coloured rocks, contain pectolite, albite, and carbonate. The minerals within the folia are late as they extend outward and partially replace the fine-grained schist.

In limited areas, along the margins of the tectonic inclusions, the albite–crossite schist grades into a much denser rock (S.G. $= 3{\cdot}10$) containing essentially fibrous, green, Jd-rich pyroxene intergrown with albite and banded by opaque stringers containing sphene. X-ray and optical determinations on this fibrous pyroxene suggest a composition similar to the analysis No. 3 in Table 1 (approximately 75 per cent Jd+25 per cent Ac, Di, He). Cross-joints developed in the green jadeite–albite schists are filled with white jadeite (Pl. 1). The joints form in the '*a*–*c*' plane of deformation and show no differential movement. The jadeite crystallized inward from the joints and in the central portions may be intergrown with low albite. Later shearing movements have offset the veins in some areas and albite is found healing shears and replacing the jadeite. Analcime is found replacing both the jadeite and albite in restricted areas within the veins (Fig. 5). The contacts between the jadeite–albite veins and the schist are sharp and replacement of schist by the vein material was not observed.

Tracing the jadeite–albite-filled '*a*–*c*' joints from the edge of the tectonic inclusion inward, jadeite is replaced by albite and zeolites. Natrolite and thomsonite predominate inward and form radial crystals that grow outward from the vein walls. Fibrous pectolite infills the interstices between the larger zeolite crystals.

Other tectonic inclusions within the area containing jadeite reveal the same pattern of jadeite deposition. These inclusions are also dominantly albite-rich schists lacking in free quartz and with greater or lesser amounts of stilpnomelane, crossite, and acmite. In the large inclusion (Fig. 2, Locality No. 1) small jadeite masses are present within the centre of the mass as well as along its margins. These all show transition from albite–crossite–stilpnomelane schists into green jadeite–albite rocks and there can be little doubt that this transformation took place with minor metasomatism.

Pod-like jadeite deposits. These bodies form bold resistant outcrops and have

a very indistinct contact with the serpentine country rock (Fig. 2, Locality No. 3; Fig. 6). Following the usage of Brothers (1954) these bodies could also be classed as tectonic inclusions; however, their small size and peculiar zonation place them in a different category from the schist inclusions previously described.

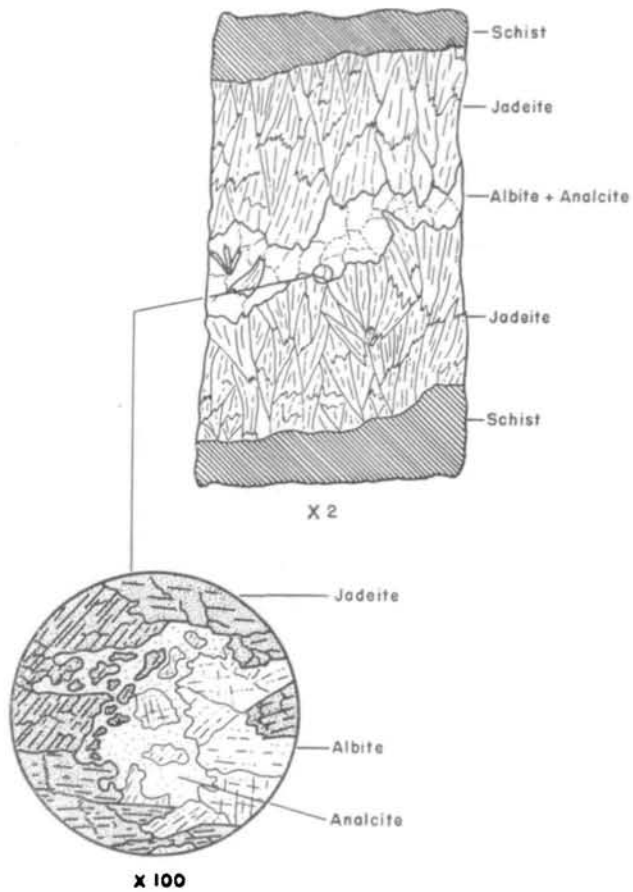

FIG. 5. Sketch of jadeite vein showing relations between jadeite, albite, and analcite. The enclosing schist contains green jadeite and albite. Locality No. 2 shown in Fig. 2.

Near the contact, the serpentine is sheared into ellipsoidal fragments that are veneered by a thin film of black, glassy antigorite completely surrounding bodies of chrysotile. This gives way to an earthy, weathered, chloritic material at the contact, showing extreme cataclastic movement. The outer rim of the pod is a tough, greenish to brown, fine-grained rock composed essentially of fibrous pectolite, hydrogarnet, thomsonite, and sphene. The sphene is concentrated in distinct bands reminiscent of bedding or schistosity, although the other minerals within the rock form an extremely fine matte of interlocking grains.

This outer zone grades imperceptibly into a similar rock that is brownish,

with a cavernous weathered surface. It also is composed of an interlocking matte of thomsonite, pectolite, and hydrogarnet, with late veins of hydrogarnet. Irregular patches of carbonate, showing a peculiar sieve-texture, are common throughout the rock. Again, sphene forms segregated bands that appear to be

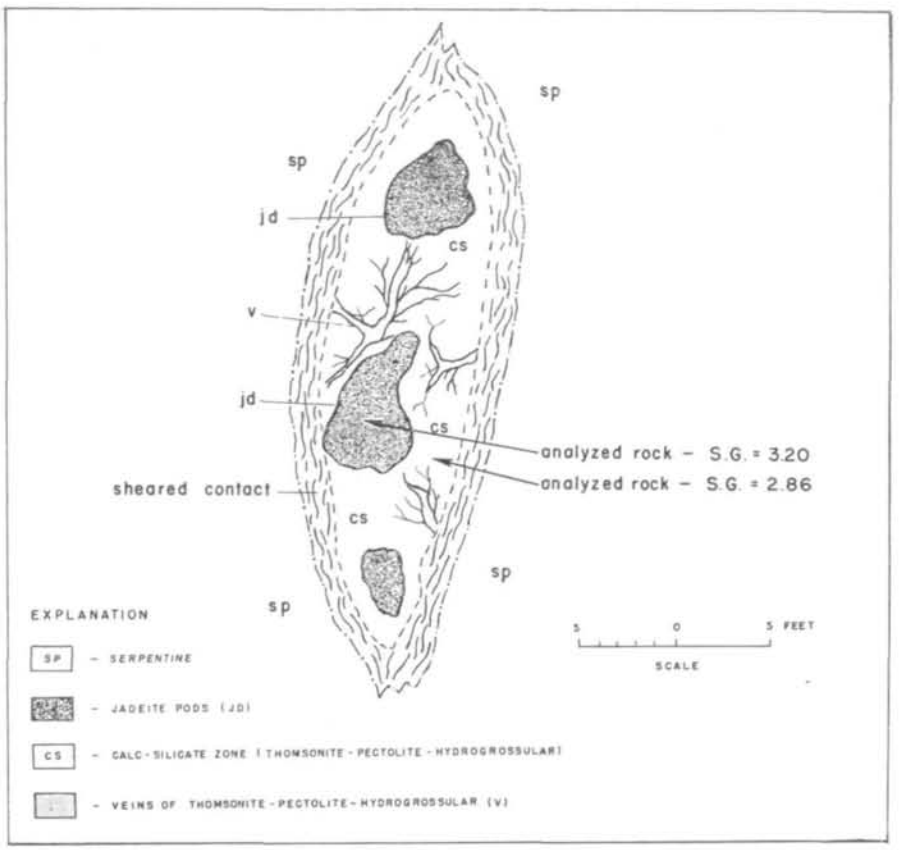

FIG. 6. Geological sketch-map of pod-like jadeite body, Locality No. 3, Fig. 2 (105-RGC-58).

relicts of original bedding. Pale greenish-brown chlorite is concentrated along shear planes. Within this calc–silicate zone, irregular white veins and pockets permeate and replace the greenish-brown rock (Fig. 6). These late veins contain mostly thomsonite with small blebs of natrolite as a mosaic aggregate. Pectolite crystallizes in isolated fibrous bundles associated with irregular patches of hydrogarnet. The compositions of the hydrogrossular from this rock were given in Table 5. The zone of hydrated calcium–aluminium silicates grades into a central pod of jadeite. Where the two zones meet, there is an area, several inches wide, of interpenetrating jadeite and calc–silicates. Although some replacement of jadeite is noted within an inch of this contact, no replacement of jadeite was found extending into the jadeite core.

The core is almost monomineralic, except for small veinlets of zeolites and

biotite. Small but persistent clots of native copper are present throughout the jadeite core. No apparent structures can be observed in this core; however, when large slabs are cut, a crude banding or schistosity is revealed. This banding is crumpled and tightly folded, similar to that observed in the albite–crossite–acmite schist. The banding is not continuous, as fracturing has brecciated this material and it has later been healed by white jadeite. Two generations of jadeite can be distinguished in the core: (1) Green jadeite is dominant in the brecciated fragments that show banding. Here the jadeite has a cataclastic texture and is crowded with minute inclusions that give it a dirty appearance. (2) White jadeite forms in and around the brecciated green jadeite as veinlets healing the core into a compact mass. The late white jadeite is coarsely crystalline and free of inclusions.

Optical constants determined for the green jadeite indicate considerable solid solution of Di–Ac–He ($\gamma = 1{\cdot}679$, $Z \wedge c = 40°$, $2V = 66$–$86°$ (+), $r > v$ extreme, birefringence = 0·004), whereas those for the white jadeite are similar to those found for the analysed vein jadeite (Table 1, No. 1 $\gamma = 1{\cdot}666$, $Z \wedge c = 34°$, $2V = 70°$ (+), no dispersion, birefringence = 0·012). The early green jadeite is characterized by a strong dispersion and lower birefringence, whereas the late white jadeite shows no dispersion and has a much higher birefringence. This striking difference between the early green jadeite and the late white jadeite is consistent for all the specimens examined in the Clear Creek area.

Six pod-like masses have been found within the area shown by Locality No. 3, Fig. 2. These bodies are quite similar in size; however, the calc–silicate zone as described for the body shown in Fig. 6 is completely lacking in some of the other pods. Banding is well-developed in some bodies but less so in those bodies that have been brecciated and healed by white jadeite.

The zoning, and to a certain extent the shape, are similar to those pods described by Lacroix (1930) from Tawmaw, Burma, and to the Kotaki deposits, Japan, discussed by Iawo (1953) and Shido (1958). The Tawmaw occurrence has a central zone of jadeite followed by albite–jadeite and albite zones that grade outward into amphibolite at the serpentine contact. The Kotaki bodies exhibit similar zoning, with a central core of albite and some free quartz followed by a thin rim of jadeite which in turn gives way to an amphibolite zone at the serpentine contact.

The association of pods with larger tectonic inclusions and the relict banding of these bodies indicate a probable common source rock for all the jadeite-bearing rocks in the Clear Creek area. The chemical composition, as discussed next, provides further evidence of this relationship.

CHEMISTRY OF THE JADEITE-BEARING ROCKS

From the previous discussions concerning the mineralogy of the jadeite-bearing rocks and the associated rocks, it is apparent that their chemical composition is indeed unusual. Table 8 presents analyses of three selected rocks

representative of the Clear Creek area, two graywackes of the Franciscan formation, and two quartz keratophyres from the Del Puerto volcanics Franciscan formation of Maddock (1955). The schists characteristic of the tectonic inclusions are represented by the albite–crossite schist (No. 3). The variation between the

TABLE 8

*Chemical and spectrographic analyses of jadeite-bearing and associated rocks**

	1	2	3	4	5	6	7
	Chemical analysis						
SiO_2	57·1	37·2	64·8	77·08	68·04	68·2	72·9
Al_2O_3	20·9	13·8	15·8	12·43	12·09	13·0	11·3
Fe_2O_3	2·3	1·3	1·6	1·48	3·81	1·6	1·1
FeO	0·63	3·6	1·8	0·55	3·21	2·7	2·8
MgO	1·4	2·6	1·7	0·23	1·97	2·4	2·7
CaO	2·6	25·9	2·3	0·88	3·41	2·0	0·60
Na_2O	13·3	2·8	9·8	6·13	5·04	2·2	3·8
K_2O	0·09	0·48	0·40	0·15	0·00	2·2	0·90
H_2O^+	0·35	6·3	0·52	0·92	1·89	3·2	2·2
H_2O-	0·12	0·38	0·12	0·31	0·54	0·50	0·39
TiO_2	0·46	0·90	0·49	0·22	0·46	0·62	0·56
P_2O_5	0·04	0·00	0·07	0·02	0·05	0·10	0·12
MnO	0·07	0·14	0·10	0·07	0·10	0·08	0·20
CO_2	0·25	0·59	0·36	—	—	1·00	0·15
SO_3	—	< 0·05	—	—	—	—	—
BaO	—	3·4	—	—	—	—	—
TOTAL	99·61	99·39	99·86	100·47	100·61	99·80	99·72
	Quantitative spectrographic analysis						
Co	0·0008	0·0009	0·0008	—	—	0·0008	0·0010
Ni	0·0026	0·0037	0·0026	—	—	0·0069	0·0082
Cr	0·0066	0·010	0·0066	—	—	0·012	0·014
Zr	0·013	0·022	0·013	—	—	0·016	0·014
Sr	0·030	0·045	0·030	—	—	0·0072	0·0029
Ba	0·25	†	0·25	—	—	0·062	0·086
B	0·002	0·31	0·002	—	—	0·008	0·007
S.G.	3·20	2·86	2·75	—	—	2·75	2·62

* Analyses 1, 2, 3, 6, and 7 are Rapid rock determinations as described in U.S. Geol. Survey Bull. 1036-C. Analysts: Paul L. D. Elmore, Ivan H. Barlow, Samuel D. Botts, Marvin D. Mack. Quantitative spectrographic analyses by Harry Bastron.
† Ba determined gravimetrically.

1. Jadeite core from pod (105-RGC-58-3) (Fig. 6).
2. Pectolite–thomsonite–hydrogrossular rock from jadeite-bearing pod (105-RGC-58-2) (Fig. 6).
3. Albite–crossite schist from jadeite-bearing tectonic inclusion (54-RGC-58-6) (Fig. 4).
4. Quartz keratophyre, Franciscan formation Del Puerto volcanics of Maddock (1955), Mt. Boardman quadrangle, California (analysis from Dr. Maddock, 88-I-1; R. Klemen, analyst).
5. Quartz keratophyre, Franciscan formation Del Puerto volcanics of Maddock (1955), Mt. Boardman quadrangle, California (analysis from Dr. Maddock, 88-I-2; R. Klemen, analyst).
6. Quartz–jadeite–lawsonite–sericite schist (metagraywacke) from Franciscan formation, Angel Island, San Francisco Bay, California (80-RGC-58).
7. Graywacke from Franciscan formation, Angel Island, San Francisco Bay, California (80-RGC-58-1).

jadeite core (No. 1), and the calc–silicate rim (No. 2) are clearly shown by these analyses. For comparison, a normal graywacke (No. 7) and a metagraywacke (quartz–jadeite–lawsonite–sericite schist, No. 6) from the same locality in the Franciscan formation are included.

Rocks from the Clear Creek area are distinctly low in silica and enriched in sodium. The albite–crossite schist is similar to the monomineralic jadeite core, each showing approximately a 1 : 1 molecular ratio of Na_2O to Al_2O_3. In contrast,

the calc–silicate zone surrounding the jadeite pods is enriched in CaO and low in Na_2O.

The relations between the Clear Creek rocks, those characteristic of the Franciscan, and those from other jadeite localities must be made clear before an ultimate source rock can be established. Fig. 7 presents a triangular diagram of

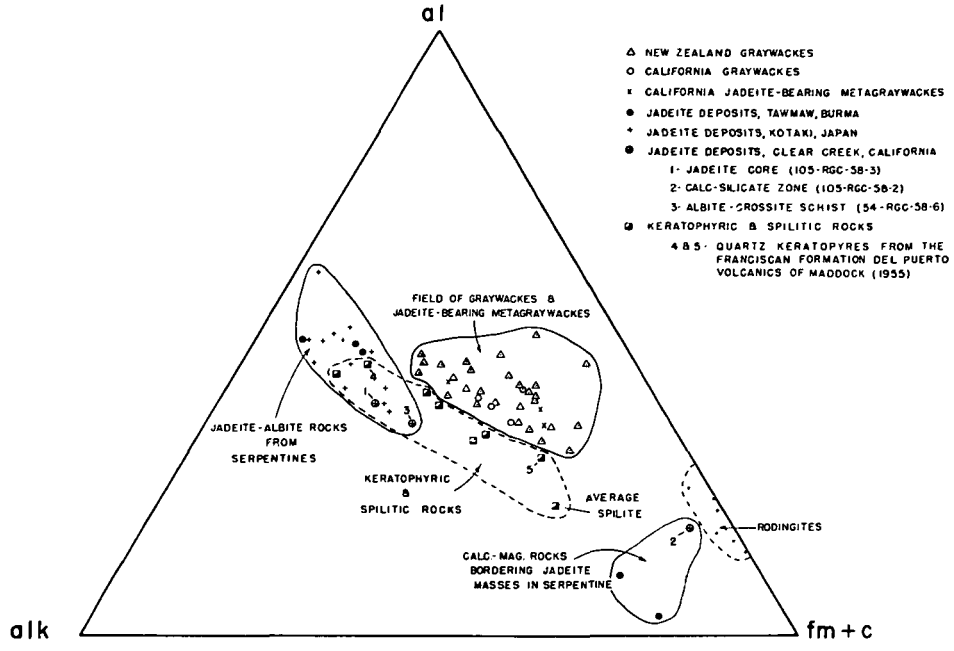

FIG. 7. Triangular diagram of Niggli values for jadeite-bearing and associated rocks $\Sigma\,[al+alk+(fm+c)] = 100$.

Descriptions and sources of plotted rock analyses:

New Zealand graywackes. Twenty-eight analyses of lower Mesozoic, Palaeozoic, and Precambrian graywackes (Reed, 1957).

California graywackes and metagraywackes. Seven analyses. (Davis, 1918; Taliaferro, 1943; Bloxam, 1956; two analyses, Table 8).

Jadeite deposits, Tawmaw, Burma. Five analyses representative of the zones in the Tawmaw Dike (Lacroix, 1930).

Jadeite deposits, Kotaki, Japan. Thirteen analyses of albitites associated with jadeite-bearing rocks (Iwao, 1953).

Keratophyric and spilitic rocks. Five selected analyses representing highly sodic varieties (Benson, 1915; Park, 1946; Dewey and Flett, 1911; Sundius, 1930; Norin, 1937; two analyses, Table 8).

Rodingites. Analyses taken from Bloxam (1954), Baker (1959), Marshall (1911), Grange (1927), and Miles (1950).

Jadeite deposits, Clear Creek, California (three analyses, Table 8).

The field boundaries are arbitrary and are not meant to be restrictive in a chemical sense.

Niggli values determined for these rock types. Here the values *al*, *alk*, *fm*, and *c* are used to characterize each analysed rock. The values *fm* and *c* are combined so that $\Sigma[al+alk+(fm+c)] = 100$.

Graywackes from New Zealand (Reed, 1957) and California (Taliaferro, 1943; Bloxam, 1956) are plotted along with three California jadeite-bearing metagraywackes (Bloxam, 1956) to establish the apparent homogeneity of this group of rocks. Available and reliable rock analyses of jadeite-bearing and associated rocks from the Tawmaw, Burma, occurrence (Lacroix, 1930) and the Kotaki District, Japan (Iwao, 1953), are also plotted. To complete the picture, two quartz keratophyres from the Franciscan formation Del Puerto volcanics

of Maddock (1955) in the Mt. Boardman quadrangle, California, are included with other spilitic and keratophyric rocks typical of these orogenic zones.

The comparison of Niggli values for the jadeite-bearing rocks, when plotted in this fashion, reveals three distinct groups that are related to their mode of occurrence. Jadeite deposits within serpentine masses from Burma, Japan, and California are characterized by nearly equal amounts of *al* and *alk* with very low *fm*+*c*. These are considered as comprising a distinct group. A second group is formed by the peculiar Ca–Mg silicate zones surrounding the jadeite–albite masses in serpentine. Jadeite is not reported in these zones from Burma (Lacroix, 1930) or Japan (Iwao, 1953); however, these rocks represent intermediate reaction zones between the jadeite masses and the enclosing serpentine. Most of the rocks from the Kotaki District, Japan, are described as albitites and none of those analysed is truly representative of the jadeite masses. Analysed rocks from Tawmaw, Burma, however, include both the jadeite and albitite zones.

A third group is formed by the California and New Zealand graywackes, and the jadeite-bearing metagraywackes of California. Metamorphism of California graywackes to quartz–jadeite–lawsonite schists produces no apparent change in bulk composition, as shown by the coherence of this third group on the diagram. It seems clear, then, that jadeitic metagraywackes represent a distinct metamorphic facies. Reed (1958) has shown very clearly that regional metamorphism of the New Zealand graywackes, similar in composition to California graywackes, gives rise to schists typical of the greenschist and amphibolite facies. These same graywackes of the New Zealand geosyncline are characterized by the zeolite facies in less intensely metamorphosed areas (Coombs *et al.*, 1959).

In contrast, the albite–crossite schist within the New Idria serpentine mass has an unusual composition. Extensive metasomatism of these schists is not supported by field and petrographic evidence. Preservation of original bedding planes attests to their sedimentary origin; however, almost complete reconstitution of the minerals precludes a possible clue as to whether the source-material was detrital and/or volcanic. Close similarity in composition between the Franciscan Del Puerto keratophyres and other keratophyres described by Benson (1915), Norin (1937), and Park (1946), and the albite–crossite schist suggests that they may have been derived from keratophyric pyroclastic marine sediments. The extremely low K_2O content of the Clear Creek schists sets them apart from other Na_2O-rich sediments such as the Gowganda Precambrian argillites (Pettijohn & Bastron, 1959) or the Tibet hornstones (Norin, 1937). Even though these argillites and hornstones are exceptional for their high Na_2O/K_2O ratio, the total K_2O content is much greater than that found in the schist of the Clear Creek area.

It is difficult to establish a direct connexion between the pod-like jadeite occurrences and their pre-metamorphic precursors. However, a plot of the SiO_2-Al_2O_3–Na_2O molecular ratios for the Franciscan Del Puerto quartz keratophyres, the albite–crossite schist, and the jadeite cores (from Table 8) illustrates

a possible relation between these rocks (Fig. 8). By progressive loss of SiO_2, the keratophyric rocks could easily attain a composition favourable for the formation of jadeite. Desilication could be effected during and after tectonic emplacement of keratophyric material within serpentine. The unusual zoning suggests this possibility, as these small bodies may have differentiated during metamorphism of keratophyric tuff. The striking resemblance in composition between the jadeite core and albite–crossite schist gives further credence to this possibility.

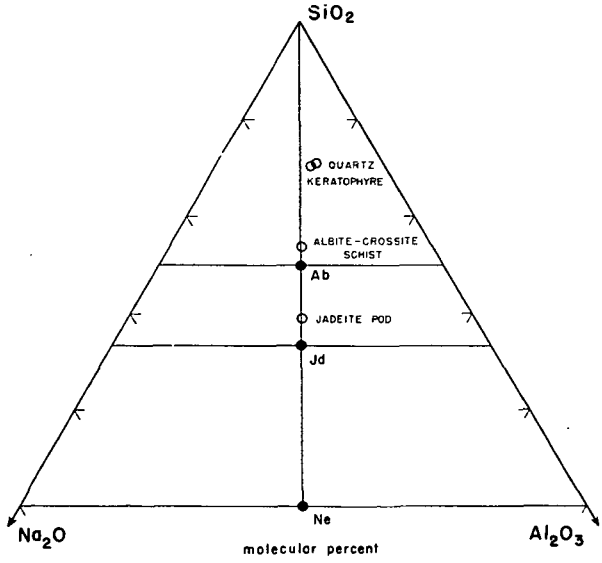

FIG. 8. Plot showing the relations between the phases Ab (albite), Jd (jadeite), and Ne (nepheline) and the molecular ratios of SiO_2–Na_2O–Al_2O_3 in the Franciscan formation Del Puerto keratophyres of Maddock (1955) and the Clear Creek rocks.

The outer calc–silicate zone in many respects resembles (Fig. 7) the mineralogy of rodingites (Grange, 1927; Bloxam, 1954; Baker, 1959; Miles, 1950). It is generally considered that hydrothermal calcium-rich solutions within serpentines alter gabbroid rocks into calc–silicate masses of hydrogarnet, idocrase, and diopside (rodingites) during the process of serpentinization (Benson, 1915; Bloxam, 1954). The outer margins of jadeite pods may well have developed in a similar manner during the period of metamorphism of the keratophyric inclusions to jadeite. The high boron content and increase in chromium over that in the jadeite core are interpreted as evidence for this reaction (Table 8). Enrichment of boron in serpentines has been demonstrated by Faust *et al.* (1956) and they consider that this enrichment takes place during serpentinization. The boron content of six serpentine samples from the New Idria mass ranges from 0·01 to 0·05 per cent boron by spectrographic analyses, whereas the jadeite core shows 0·002 per cent and the albite–crossite schist contains less than 0·002 per cent boron. This boron concentration demonstrates that formation of the jadeite

core and calc-silicate border may have been contemporaneous with, or later than, the process of serpentinization.

The clustering of the larger tectonic inclusions and pods in the Clear Creek area indicates that during serpentinization or shortly thereafter, keratophyric tuff blocks of varying sizes were emplaced tectonically. The smaller bodies undergoing more intense metamorphic reaction with serpentine have become zoned, whereas the larger bodies show only local reaction with the enclosing serpentine.

In considering the Burmese, Japanese, and Californian occurrences, a striking parallelism is observed in their chemical composition and zoning. All these occurrences show a zoning which, in a general way, follows the same pattern. The central core is usually albite and/or jadeite intergrown or as distinct bands. This central core is surrounded by a rim which is characteristically enriched in Ca–Mg silicates. The mineralogy for these three occurrences varies considerably from one to the other; however, the bulk composition of each zone demonstrates a remarkable consistency, i.e. Na–Al-rich cores and Ca–Mg-rich borders. Rather than call on exotic intrusives or desilicification of granitic intrusives (cf. Lacroix, 1930; Chhibber, 1934; Bleeck, 1907) to explain these deposits, it seems much more reasonable to assume an original composition in keeping with the common associates of these orogenic zones; i.e. serpentine–graywackes, spilites–keratophyres.

The mutual chemical and geological conformity between the Californian, Japanese, and Burmese jadeite deposits manifests a common genesis. It is proposed that these deposits developed from keratophyric or spilitic inclusions tectonically emplaced within serpentine. Following emplacement, metamorphic reaction at depth, between serpentine and inclusions, provided an environment that allowed the stable formation of jadeite.

MINERAL FACIES AND THEIR RELATION TO THE FORMATION OF JADEITE

Important to a discussion regarding the origin of jadeite in these deposits is a clear description of the associated minerals that appear to be in equilibrium with jadeite, and of those that have formed either earlier or later than the jadeite. It is apparent from the textural relations in many thin sections studied that equilibrium may never have been attained during the period of jadeite crystallization; however, where jadeite coexists with other minerals and replacement one by the other was not suggested by their textures, it is assumed that the coexisting minerals closely approached equilibrium.

As shown in a previous section, jadeite is found in two distinct environments: (1) small areas in albite–crossite schist inclusions, and (2) pod-like bodies associated with calc-silicates.

Within the schist, green jadeite was not replaced by albite, nor was it found replacing acmite or glaucophane. The stable assemblage is:

Green jadeite (5–25 per cent Ac–Di–He)+low albite (An_{0-2})

As the small areas of green jadeite–albite schists can be traced into albite–crossite schists, it is assumed that the formation of jadeite was accomplished by metamorphism of the albite–crossite schist. Veins of white jadeite (98 per cent Jd) cutting the green jadeite–albite schist are clearly later, and again show the following stable assemblage:

White jadeite (98 per cent Jd)+low albite (An_{0-2})

Within the veins, low albite (An_{0-2}), analcime, and zeolites are found replacing the jadeite–albite assemblage. These joints may represent low-pressure zones similar to those developed in boudins (Ramberg, 1955) and contain 'sweated out' silicates and hydrous phases representing an accumulation of available liquid within the low-pressure zone.

Experimental studies on the stability of the mineral assemblages present in the Clear Creek area have been under intensive study during recent years, and therefore a discussion of the natural assemblages, in the light of the experimental findings, is necessary. The reactions previously studied, together with the relevant references to some of the experimental work and thermodynamic relations, are given below:

$$\text{nepheline}+\text{albite} = 2\ \text{jadeite} \tag{1}$$

(Robertson *et al.*, 1957; Adams, 1953; Yoder & Weir, 1951)

$$\text{analcime} = \text{jadeite}+\text{water} \tag{2}$$

(Griggs & Kennedy, 1956; Fyfe & Valpy, 1959)

$$\text{albite} = \text{jadeite}+\text{quartz} \tag{3}$$

(Robertson *et al.*, 1957; Fyfe & Valpy, 1959; Birch & LeComte, 1960)

$$\text{analcime} = \text{nepheline}+\text{albite}+\text{water} \tag{4}$$

(Yoder, 1954, 1950*a*; Fyfe & Valpy, 1959)

The complete absence of quartz from the Clear Creek jadeite deposits eliminates reaction (3) from this discussion or it would have to be assumed that silica was removed from the system during jadeite formation. Kracek *et al.* (1951) have determined the thermodynamic properties of jadeite and the other minerals involved in reactions (1) and (2). As shown by their data, the formation of jadeite is favoured by a silica-deficient environment because the free energy change for reaction (3) is positive ($\Delta F = +1{\cdot}60$ K cal at 298° K), whereas for reaction (1) it is negative ($\Delta F = -1{\cdot}15$ K cal at 298° K). Considering the composition of the albite–crossite schist, and the lack of quartz both during the formation of jadeite and during its inversion to albite and/or analcime, reactions (1) and (2) more nearly represent the composition during the Clear Creek jadeite formation. It must be stated that nepheline was not identified in any of the specimens from the area, but for this discussion the nepheline molecule could be contained within natrolite.

Assuming that the bulk composition of the jadeite-bearing rocks was derived

by desilicification of keratophyric material within the serpentine mass, a diagram can be constructed to demonstrate the sequence (Fig. 9). All bulk compositions of the rocks plotted on the diagram include SiO_2, Al_2O_3, Na_2O, and H_2O. These oxides make up 87 to 90 per cent (by weight) of the total rock composition with $Na_2O:Al_2O_3$ (molecular per cent) very nearly 1:1 in each case (see Fig. 8). The

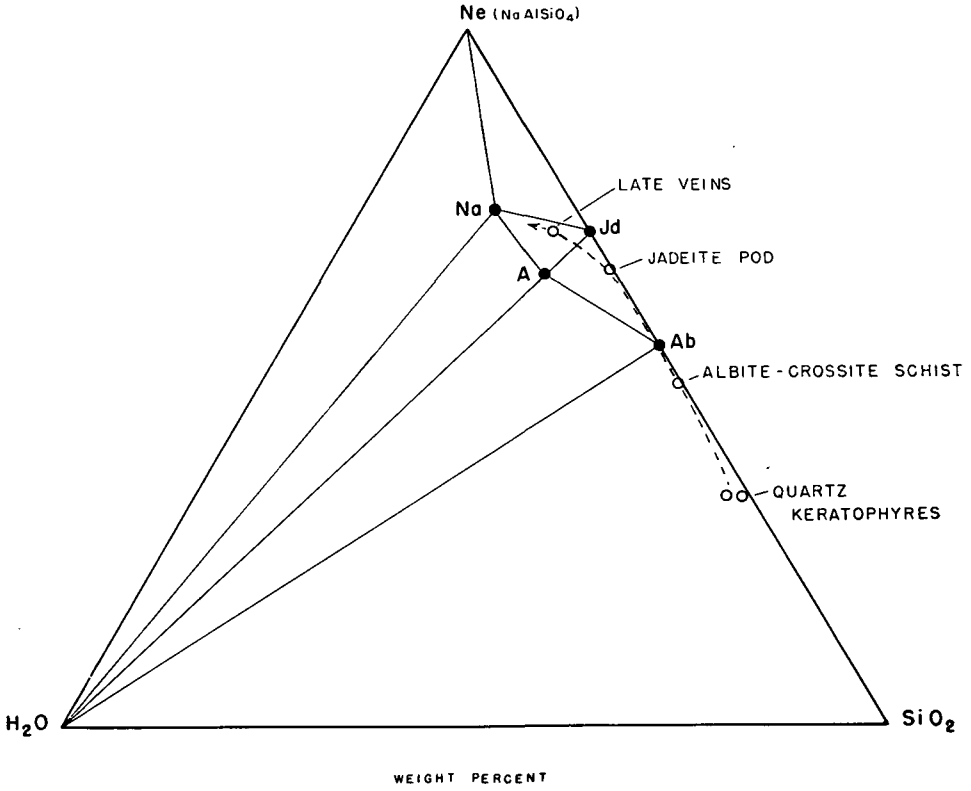

FIG. 9. Triangular plot illustrating the relations between bulk compositions of the jadeite-bearing rocks and the stable assemblages. Ne (nepheline), Na (natrolite), A (analcime), Jd (jadeite), Ab (albite). Weight per cent.

phases expected with each compositional type are included on the diagram. The keratophyres, albite–crossite schists, and jadeite pod all fall on or near the SiO_2–Ab–Jd–Ne line. An estimated composition of the zeolite–jadeite veins in the schist bodies is plotted to illustrate their high water and low silica content. Modal analysis of the keratophyres shows 53–58 per cent albite and 35–38 per cent quartz (?); the remainder consists of varying amounts of chlorite, augite, and opaque minerals (Maddock, 1955).

The phases Ab ($Na_2O.Al_2O_3.6SiO_2$), Jd ($Na_2O.Al_2O_3.4SiO_2$), A ($Na_2O.Al_2O_3.4SiO_2.H_2O$), Na ($Na_2O.Al_2O_3.3SiO_2.2H_2O$), and H_2O gas, all lie within a plane of the system SiO_2–Al_2O_3–Na_2O–H_2O where $Na_2O:Al_2O_3$ is 1:1. Morey (1957) has discussed in detail, on a theoretical basis, possible univariant *P–T*

curves and invariant points within this same system. Following his reasoning, the mineral assemblages associated with the Clear Creek jadeite are plotted in the triangular diagram of Fig. 9. The coexisting mineral phases most commonly observed are as follows; these may be stable or metastable assemblages:

(1) Jd; (2) Jd+Ab; (3) Ab; (4) Ab+Jd+A; (5) Jd+A+Na.

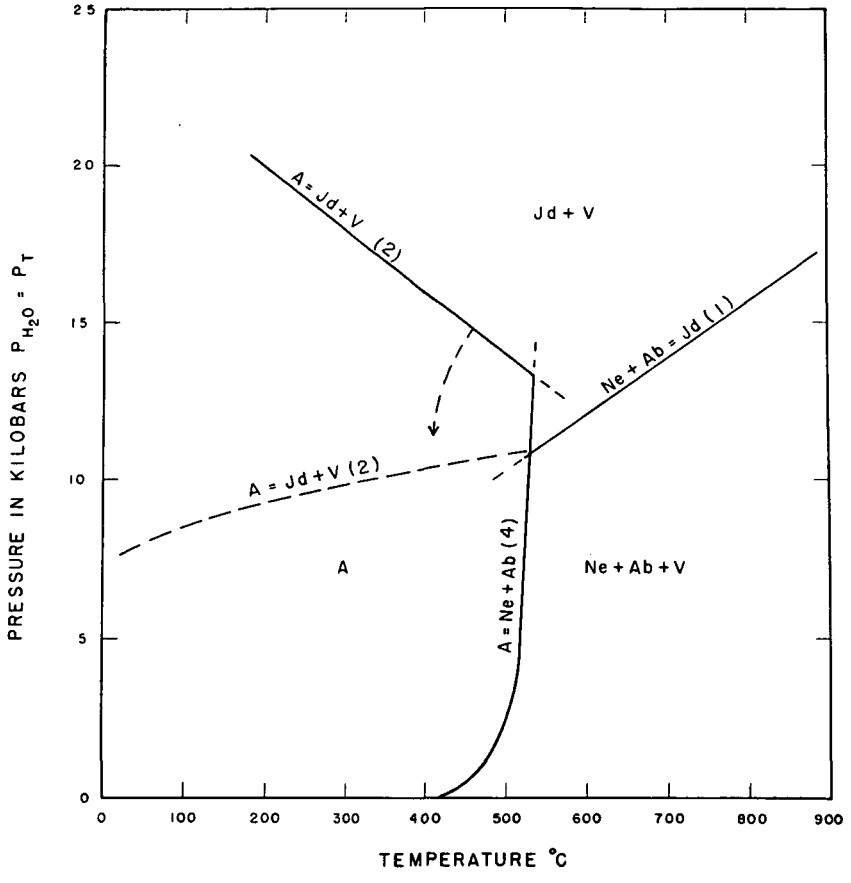

FIG. 10. Equilibrium lines for reactions (1) Robertson *et al.* (1957), (2) Griggs & Kennedy (1956), Fyfe & Valpy (1959), (4) Yoder (1954).

Jd+Ab coexisted, in the early stages, and as crystallization continued Jd became the dominant phase with a minor development of Jd+Ab+A. At this time the bulk composition could have been within the triangle Jd–Ab–A and near the Jd–Ab tie-line. The appearance of A suggests local variations in water pressures or temperatures. The experimental stability of analcime, as shown in Fig. 10, indicates that it is stable up to 500° C when $P_{H_2O} = P_{total}$. Yoder (1954) has shown that this stability limit of analcime is reduced to 400° C when $P_{H_2O} = 1$ atm. For reaction (2), Fyfe & Valpy (1959) have suggested that the equilibrium curve (Fig. 10) may assume a positive slope at low temperatures.

Therefore at low temperatures, when $P_{H_2O} < P_{total}$, jadeite may form more readily as the analcime field of stability becomes restricted. Nepheline is not found in the Clear Creek deposits; however, natrolite is found sparingly replacing jadeite and analcime or coexisting with analcime. Na+Jd+A could coexist when the bulk composition lies within the triangle Na–Jd–A. By changing this composition to lie within the triangle A–Jd–Ab, Na would not be stable and Ab would appear. Natrolite and albite were not found together in any of the deposits.

Jadeite and albite may exist at moderate temperatures and high pressures (Fig. 10), as shown by Robertson *et al.* (1957). Replacement of this pair by analcime, and in the later stages by natrolite and other zeolites, suggests either a low silica environment, increase of H_2O, or lower pressures and temperatures. The amount of H_2O determines to a large extent the mineral assemblages and H_2O undoubtedly must have been present in varying amounts during the formation of the Clear Creek deposits. Fyfe & Valpy (1959) have suggested that jadeite may form at low temperatures and high pressures if the water pressure is less than the total pressure; however, there is no way of determining the water pressures relative to the total rock pressure for the Clear Creek deposits.

The mineral assemblage formed in the calc–silicate zone surrounding the jadeite pods provides us with a means of comparing the mineral facies developed in calcium–aluminium silicate rock and the jadeite core facies. It has been said that the calc–silicate zone formed as a reaction between the pod and fluids present within the serpentine. Whether this reaction took place during serpentinization or at the time of jadeite formation is not clear. The composition of the calc–silicate and jadeite zones is so distinctly different (Table 8) that the calc–silicate zone cannot be regarded as a retrogressive metamorphic equivalent of the jadeite core. The minerals now present in the calc–silicate zone are considered to have formed under the same *P–T* conditions as those giving rise to the jadeite core. The following minerals are found to coexist in this zone:

pectolite–thomsonite–hydrogarnet–carbonate

The mineral phases have been plotted on a triangular diagram with CaO–SiO_2–Al_2O_3 at the apexes, together with a point representing the approximate composition of the rock containing these minerals (Fig. 11). Experimental work on the stability of grossularite–hydrogrossular by Flint *et al.* (1941), Yoder (1950*b*), and Carlson (1956) allows for some speculation on the conditions for formation of hydrogrossular in this rock. Yoder has shown that grossularite in the presence of water at elevated temperatures is unstable and inverts to hydrogrossular. Above 750° C grossularite–hydrogrossular solid solutions are unstable and invert to gehlenite–wollastonite–anorthite in the absence of quartz. Carlson (1956) extended Yoder's curve and has defined the relationships between temperature of formation and composition, for the hydrogarnets. The silica content of hydrogrossular increases with temperature up to 800° C, 1,020 atm, at which

point grossularite becomes stable, whereas fully-hydrated hydrogrossular is stable at 220°–226° C, 1,020 atm. Assuming that the hydrogarnets associated in the calc-silicate zone formed contemporaneously with the jadeite core, a minimum temperature of formation can be estimated. To make such an assumption,

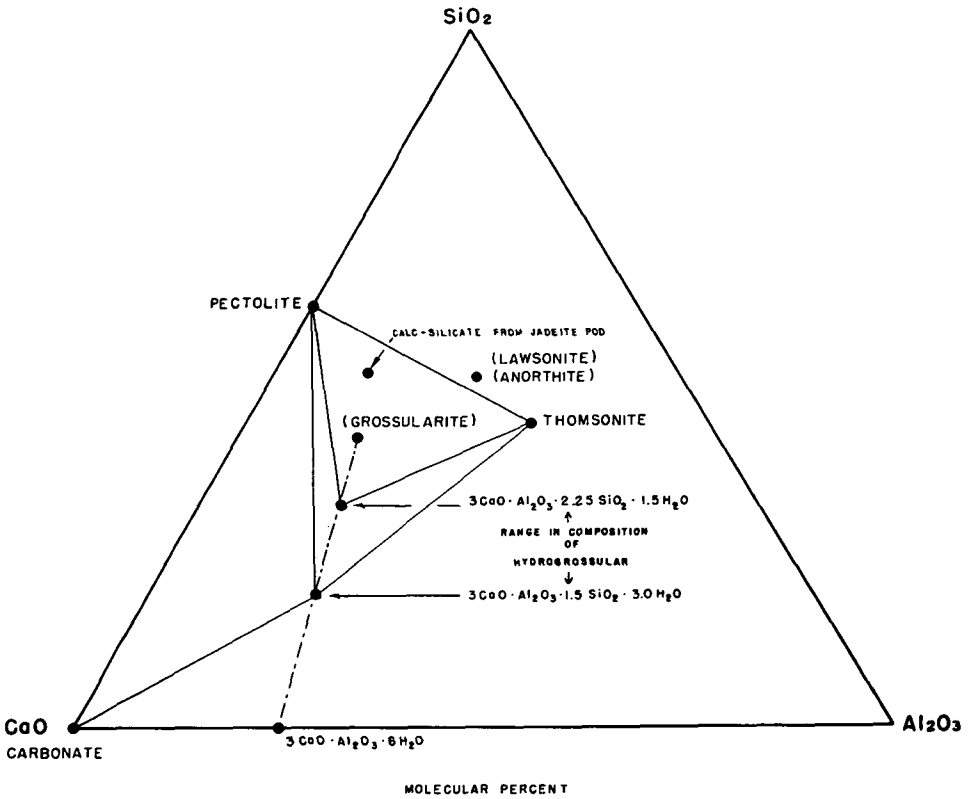

FIG. 11. Triangular diagram of CaO, Al_2O_3, SiO_2 system illustrating the relations of the minerals present in the calc-silicate rock of the jadeite pods. The composition of the calc-silicate rock plotted is from Table 8 and the minerals contained are pectolite–hydrogrossular–thomsonite–carbonate. Only a few tie-lines are shown.

it would be necessary to exclude the possibility of silica loss during the hydrogarnet formation. Pistorius & Kennedy (1960) have shown experimentally that the presence of quartz might affect the stability of grossularite–hydrogrossular; however, it is doubtful that equilibrium conditions were obtained, because the unit cell variations of their synthesized hydrogarnets suggest strong compositional variation. With these restrictions in mind, hydrogarnets from the calc-silicate zone may have formed at temperatures ranging from 240°–360° C, and hydrogarnets in late veins suggest temperatures between 260° and 300° C. These reactions are not necessarily pressure-dependent, as demonstrated by Yoder (1950*b*) and Carlson (1956).

Further evidence on temperature and pressure conditions within the calc–silicate zone may be obtained by considering Fyfe's work (Ellis & Fyfe, 1957; Fyfe, Turner, & Verhoogen, 1958; Fyfe & Valpy, 1959; Coombs *et al.*, 1959) on the stability of thomsonite–lawsonite–anorthite. As shown in Fig. 11, lawsonite or anorthite could be expected to form within the calc–silicate rock with a slight increase of silica content. Fyfe has suggested that thomsonite is stable below 300° C with low water pressures; with an increase in water pressure above 5,000 bars, thomsonite may invert to lawsonite. Anorthite is stable above 300° C at low water pressures and might also invert to lawsonite by a large increase in the partial pressure of water. Assuming that the bulk composition would allow the formation of lawsonite, the presence of hydrogarnet and thomsonite within the calc-silicate zone suggests that the temperatures were less than 300° C and that the pressures ranged from 5,000 to 8,000 bars.

Additional indirect evidence on the *P–T* conditions prevailing during the formation of jadeite in the Clear Creek area may be obtained by considering the reaction:

$$\text{serpentine} \rightarrow \text{forsterite} + \text{talc} + \text{vapour}$$

All the jadeite-bearing rocks lie within the serpentine and, as discussed earlier, the period of jadeite mineralization is considered to be later than, or contemporaneous with, the period of serpentinization. Bowen & Tuttle (1949, p. 459) state: 'serpentine cannot be present in any layer of the earth's crust whose temperature is normally above the decomposition temperature (500° C) under the pressure prevaling'. The serpentine, then, fixes the maximum temperature as there is no evidence for the decomposition of serpentine to forsterite+talc in the Clear Creek area.

The schists from the tectonic inclusions are classified as belonging to the greenschist or glaucophane schist facies as defined by Turner (Fyfe, Turner, & Verhoogen, 1958). As lawsonite has not been identified in these rocks and the jadeite is restricted to local areas within albite–crossite–stilpnomelane schists, it seems appropriate to place the schists in the chlorite zone of metamorphism as defined by Hutton (1940). Turner has suggested that the greenschist facies probably does not form below 300° C with P_{H_2O} between 5,000 and 10,000 bars.

If the interpretation of the mineral facies is correct in the light of experimental data, and if the observed geological relations are correct, it is suggested that these jadeite deposits developed at temperatures less than 300° C and at pressures near 5,000 bars with $P_{load} > P_{H_2O}$.

These *P–T* values are much less than have been recorded experimentally for reactions (1), (2), and (3). However, several points of difference can be cited between the experimental conditions and the reconstructed conditions found for the Clear Creek jadeite deposits; these differences may explain why jadeite develops at low temperatures and moderate pressures.

(1) The jadeite composition varies from almost pure material to as much as 25 per cent Di–Ac–He. The effect of diopside–acmite solid solution has not

been investigated for reactions (1), (2), and (3). It would seem probable that Ac solid solution in the Jd molecule could strongly affect the stability curve of jadeite and would certainly lower its stability pressure, as Ac is stable at 1 atm.

(2) As a low silica environment favours the formation of jadeite, it may be that the serpentine mass continuously captured silica during the period of jadeite mineralization. Leaching of silica from tectonic inclusions may be simultaneous with the formation of serpentine if we assume the reaction forsterite+SiO_2+H_2O = serpentine. Removal of silica during experimental synthesis of jadeite is not easily accomplished.

(3) The partial pressure of water may have been profoundly affected by the serpentine mass. If it is assumed that the formation of jadeite took place during or shortly after the period of serpentinization, the water content may have been reduced by the conversion of the ultramafic to serpentine. Thus, vein jadeite may have formed where the water phase was nonexistent or greatly reduced in quantity. As shown by Adams (1953) and Fyfe & Valpy (1959), a dry environment favours the formation of jadeite.

(4) Excluding the vein-type jadeite, the localized distribution of the other jadeite bodies and zones gives some credence to the possibility that shearing or directed pressures may be effective catalysts in causing jadeite to form. All the equilibrium studies on jadeite were made under hydrostatic pressures.

CONCLUSIONS

Formation of jadeite within the New Idria serpentine mass was restricted to large tectonic inclusions of albite–crossite schist and smaller zoned pods situated near these inclusions. Assuming that sodium was not introduced, the composition of these schists is similar to keratophyric lavas. Emplacement of the keratophyric blocks within the serpentine was accomplished during the period of orogeny when the serpentine invaded the geosynclinal sediments and volcanics of the Franciscan, at depth. Metamorphism of the keratophyric rocks developed, mainly, albite–crossite–stilpnomelane–acmite schists. Localized areas of high confining pressures along the margins of the tectonic inclusions gave rise to green jadeite–albite schists. Continuing tectonic movement and possible mobilization of a liquid rich in the jadeite molecule and low in H_2O produced cross-cutting veins of white jadeite+albite. A lowering of the water pressure could have resulted in the later replacement of albite–jadeite by zeolites. The smaller pod-like bodies may have been keratophyric blocks that reacted to a greater extent with fluids within the serpentine, giving rise to a rodingite-like calc-silicate zone surrounding the jadeite core. The Californian, Burmese, and Japanese bodies all follow the same pattern; that is, a central Na–Al silicate core grading into border zones of lower silica and sodium content and increasing in Ca–Mg silicates. It seems apparent that these bodies have reacted with fluids within the serpentine and, in so doing, a typical metamorphic differentiation

trend was developed. Similar zoning has been recognized in serpentines both at their contacts (Phillips & Hess, 1936; Read, 1934) with siliceous country rock and for bodies within serpentine (Watson, 1953; Francis, 1955). The metamorphic reaction between serpentines and siliceous rocks is characterized by enrichment of Na–Al silicates in the central zone and outward decrease in silica and enrichment in Ca–Mg. This environment, apparently common to serpentines, favours the formation of jadeite because of the low silica and enrichment of Na and Al.

Extremely high pressures are needed to form jadeite experimentally. Robertson *et al.* (1957) suggest a pressure of 15,000 bars and temperatures between 500° and 700° C to allow the ready formation of a jadeite–albite assemblage. If the assumption is made that these pressures and temperatures are attained only by depth of burial, it is necessary to allow 37 km of depth before these *P–T* conditions are satisfied (ibid., 1957). In reconstructing the hypothetical depth of burial for the serpentine and contained jadeite deposits in the New Idria area, from stratigraphic data given by Reed (1951), it is found that a range from 9 to 12 km appears feasible.

This reconstruction is based on the assumption that the emplacement of the serpentine into the geosynclinal sediments and volcanics of the Franciscan coincided with the Nevadan Orogeny and that during this emplacement, tectonic inclusions derived from the geosynclinal sediments and volcanics became immersed in the serpentine. The presence of serpentine debris in Miocene sediments derived from the New Idria mass indicates that the serpentine reached the surface during this time; therefore, to attain a depth of 12 km, it has to be assumed that the serpentine was covered by the total thickness of sediments making up the Jurassic to Miocene section in the New Idria area. It therefore seems impossible that these rocks could ever have been at depths up to 37 km.

Thus one is forced to call upon a unique situation to allow the stable formation of jadeite in the upper portions of the earth's crust. Based on thermodynamic calculations of Adams (1953), it is possible to form jadeite in anhydrous conditions by the reaction nepheline+albite = 2 jadeite at approximately 240° C and 2,000 bars. The stability of crystalline OH-bearing minerals under varying *P–T* conditions dictates the P_{H_2O} to a great extent (Yoder, 1955). In a serpentine mass, almost all the water may be effectively held in the structure of the serpentine minerals. Thus at great depths, the partial pressure of water in a serpentine mass could have been small compared to the total rock pressure. The tectonic inclusions, being small in mass compared to the serpentine body, are in essence affected by this same pressure as any residual interstitial water could migrate to the serpentine and be used in the process of further serpentinization. This effective mechanism would provide an anhydrous environment and also produce very low partial water pressures, both of which favour the formation of jadeite at low temperatures and somewhat reduced total pressure.

The localized nature of jadeite in the tectonic inclusions and pod-like bodies

may be indicative of local shearing stress which could give rise to high enough pressures within these small areas to favour the formation of jadeite. However, the unique situation within the serpentine body which has produced a silica gradient away from the tectonic inclusions, combined with a dry environment, seems to be the important factor in the formation of jadeite.

Further experimental work is needed to elucidate the role of diopside–acmite solid solution and its effect on the stability of jadeite. As yet we are not able to suggest a field of stability at high pressures and low temperatures for the reactions (1) and (3). Another problem regarding the stability of jadeite is its extensive development in metagraywackes in equilibrium with quartz and lawsonite (McKee, 1958; Bloxam, 1956), within the Franciscan formation. The association of quartz with jadeite in these rocks moves us to reaction (3) where even greater pressures are needed to allow the stable formation of jadeite. Here again there is no evidence that these rocks attained depths greater than 12 km.

ACKNOWLEDGEMENTS

This problem was initiated while the author was pursuing graduate studies at Stanford University, where much of the preliminary work was completed under the guidance of Professor C. O. Hutton, to whom I am grateful for advice and counsel. Reviews by David B. Stewart and George Phair, U.S. Geological Survey, have enhanced the petrological interpretations. Hatten S. Yoder, Jr., Geophysical Laboratory, has allowed free use of his preliminary data on these deposits and ensuing discussions on the problem were of value to the author. Further discussions with Professor William S. Fyfe, University of California, on the experimental aspects of the problem, assisted in the interpretation. George S. Switzer, U.S. National Museum, kindly provided chemical analyses and specimen material for two jadeites from the Clear Creek deposits. Professor Marshall E. Maddock, San Jose State College, has allowed the writer the use of two unpublished analyses of the Del Puerto quartz keratophyres.

REFERENCES

ADAMS, L. H., 1953. A note on the stability of jadeite. *Amer. J. Sci.* **251**, 299–308.

ALDERMAN, A. R., 1936. Eclogites in the neighbourhood of Glenelg, Inverness-shire. *Quart. J. geol. Soc. Lond.* **92**, 488–530.

ANDERSON, R., & PACK, R. W., 1915. Geology and oil resources of the west border of the San Joaquin Valley north of Coalinga, California. *Bull. U.S. geol. Surv.* **603**, 220 pp.

BAKER, GEORGE, 1959. Rodingite in nickeliferous serpentinite, near Beaconsfield, Northern Tasmania. *J. geol. Soc. Aust.* **6**, Pt. 1, 21–35.

BANNO, SHOHEI, 1959. Aegirinaugites from crystalline schists in Sikoku. *J. geol. Soc. Japan*, **65**, 652–7.

BELYANKIN, D. S., & PETROV, V. P., 1941. The grossularoid group (hibschite and plazolite). *Amer. Min.* **25**, 450–3.

BENSON, W. N., 1915. The geology and petrology of the great serpentine belt of New South Wales. Part IV. The dolerites, spilites, and keratophyres of the Nundle District. Part V. The Geology of the Tamworth District. *Proc. Linn. Soc. N.S.W.* **40**, 121–73, 540–624.

BIRCH, F., & LECOMTE, P., 1960. Temperature–pressure plane for albite composition. *Amer. J. Sci.* **258**, 209–17.

BLEECK, A. W. G., 1907. Die Jadeitlagerstätten in Upper Burma. *Z. Prakt. Geol.* **15**, 341–65.

BLOXAM, T. W., 1954. Rodingite from the Girvan–Ballantrae complex, Ayrshire. *Miner. Mag.* **30**, 525–8.

BLOXAM, T. W., 1956. Jadeite-bearing metagraywackes in California. *Amer. Min.* **41**, 488–96.
—— 1959. Glaucophane-schists and associated rocks near Valley Ford, California. *Amer. J. Sci.* **257**, 95–112.
BOLANDER, L. PH., 1950. First jadeite discovery in America. *Mineralogist*, **18**, 186, 188.
BOWEN, N. L., & TUTTLE, O. F., 1949. The system MgO–SiO_2–H_2O. *Bull. geol. Soc. Amer.* **60**, 439–60.
BRIÈRE, Y., 1920. Les Eclogites françaises — leur composition minéralogique et chimique; leur origine. *Bull. Soc. franç. Minér.* **43**, 72–222.
BROTHERS, R. N., 1954. Glaucophane schists from the North Berkeley Hills, California. *Amer. J. Sci.* **252**, 614–26.
CARLSON, E. T., 1956. Hydrogarnet formation in the system lime–alumina–silica–water. *U.S. Nat. Bur. Standards, J. of Res.* **56**, 327–35.
CHIBBER, H. L., 1934. *Mineral resources of Burma.* London: Macmillan & Co. Ltd.
COLEMAN, R. G., 1954. Optical and chemical study of jadeite from California (abst). *Bull. geol. Soc. Amer.* **65**, 1241.
—— 1956. Jadeite from San Benito County, California. *Gems & Gemology*, **Fall 1956**, 331–4.
—— 1957. Mineralogy and petrology of the New Idria District, California. Unpublished thesis for D.Ph. degree. *Dissertation Abstracts*, **17**, No. 7, 1533.
COOMBS, D. S., ELLIS, A. J., FYFE, W. S., & TAYLOR, A. M., 1959. The zeolite facies; with comments on the interpretation of hydrothermal syntheses. *Geochim. et Cosmochim. Acta*, **17**, 53–107.
DAVIS, E. F., 1918. The Franciscan Sandstone. *Bull. Univ. Calif. Pub. Dept. Geol.* **11**, 22 pp.
DE ROEVER, W. R., 1955. Genesis of Jadeite by low-grade metamorphism. *Amer. J. Sci.* **253**, 283–98.
DEWEY, H., & FLETT, J. S., 1911. Some British pillow lavas and the rocks associated with them. *Geol. Mag. Lond.* **8**, 202–9, 241–8.
ECKEL, E. B., & MYERS, W. B., 1946. Quicksilver deposits of the New Idria District, San Benito and Fresno Counties, California. *Calif. J. Min.* **42**, Pt. 2, 81–124.
ELLIS, A. J., & FYFE, W. S., 1957. Hydrothermal chemistry. *Rev. Pure and Appl. Chem.* (Aust.), **7**, 261–316.
ESKOLA, P., 1921. On the eclogites of Norway. *Skr. Norske Vidensk Akad.*, I Mat.-naturv., Kl., No. **8**, 1–118.
FAUST, G. T., MURATA, K. J., & FAHEY, J. J., 1956. Relation of minor element content of serpentines to their geological origin. *Geochim. et Cosmochim. Acta*, **10**, 316–20.
FLINT, E. F., MCMURDIE, H. F., & WELLS, L. S., 1941. Hydrothermal and X-ray studies of the garnet–hydrogarnet series and the relationship of the series to hydration products of Portland cement. *U.S. Nat. Bur. Standards, J. of Res.* **26**, 13–33.
FOSHAG, W. F., 1920. Plazolite, a new mineral. *Amer. Min.* **5**, 183–5.
—— 1955. Chalchihuitl—a study in jade. Ibid. **40**, 1062–70.
—— 1957. Mineralogical studies on Guatemalan Jade. *Smithsonian Misc. Collection*, **135**, No. 5, 1–60.
FRANCIS, G. H., 1955. Zoned hydrothermal bodies in the serpentinite mass of Glen Urquhart (Inverness-shire). *Geol. Mag. Lond.* **92**, 433–47.
FYFE, W. S., TURNER, F. J., & VERHOOGEN, J., 1958. Metamorphic reactions and metamorphic facies. *Mem. geol. Soc. Amer.* **73**, 259 pp.
—— & VALPY, G. W., 1959. The analcime–jadeite phase boundary: some indirect deductions. *Amer. J. Sci.* **257**, 316–20.
GRANGE, L. I., 1927. On the 'rodingite' of Nelson. *Trans. Proc. N.Z. Inst.* **58**, 160–6.
GRIGGS, D. T., & KENNEDY, G. C., 1956. A simple apparatus for high pressures and temperatures. *Amer. J. Sci.* **254**, 722–35.
HESS, H. H., 1949. Chemical composition and optical properties of common clinopyroxenes, Part I. *Amer. Min.* **34**, 621–66.
HEY, M., 1932. Studies on the zeolites. Part II. Thomsonite (including faroelite) and gonnardite. *Miner. Mag.* **23**, 51–125.
HILDEBRAND, F. A., 1953. Minimizing the effects of preferred orientation in X-ray powder diffraction patterns. *Amer. Min.* **38**, 1051–6.
HUTTON, C. O., 1940. Metamorphism in the Lake Wakatipu region, western Otago, New Zealand. *Mem. geol. Surv. N.Z.* **5**, 90 pp.
—— 1943. Hydrogrossular, a new mineral of the garnet–hydrogarnet series. *Trans. Proc. N.Z. Inst.* **73**, 174–80.
—— 1956. Further data on the stilpnomelane mineral group. *Amer. Min.* **41**, 608–15.
IWAO, S., 1953. Albitite and associated jadeite rock from Kotaki District, Japan: a study in ceramic raw material. *Geol. Surv. Japan Report*, **No. 153**, 25 pp.
JENNINGS, C. W., & STRAND, R. G., 1958. Geologic Map of California, Olaf P. Jenkins ed., *Santa Cruz sheet, California Div. Mines.*

KAWANO, Y., 1939. A new occurrence of jade (jadeite) in Japan and its chemical properties. *J. Jap. Ass. Mineralog.* **22**, 219–25 (in Japanese).

KNORRING, O. VON, & KENNEDY, W. Q., 1958. The mineral paragenesis and metamorphic status of garnet–hornblende–pyroxene–scapolite gneiss from Ghana (Gold Coast). *Miner. Mag.* **31**, 846–59.

KRACEK, F. C., NEUVONEN, K. J., & BARLEY, G., 1951. Thermochemistry of mineral substances. I. A thermodynamic study of the stability of jadeite. *J. Wash. Acad. Sci.* **41**, 373–83.

LACROIX, M. A., 1930. La Jadeite de Birmanie: les roches qu'elle constitue ou qui'l accompagnent. Composition et origin. *Bull. Soc. franç. Minér.* **53**, 216–54.

MCKEE, BATES, 1958. Jadeite alteration of sedimentary and igneous rocks (abst). *Bull. geol. Soc. Amer.* **69**, 1612.

MACKENZIE, W. S., 1957. The crystalline modifications of $NaAlSi_3O_8$. *Amer. J. Sci.* **255**, 481–516.

MADDOCK, M. E., 1955. Geology of the Mt. Boardman quadrangle. Unpublished thesis for D.Ph. degree, Univ. of Calif.

MARSHALL, P., 1911. The geology of the Dun Mountain Subdivision, Nelson. *Bull. geol. Surv. N.Z.* **12**, 29–40.

MIELENZ, R. C., 1939. The geology of the southwestern part of San Benito County, California. Unpublished thesis for D.Ph. degree, Univ. of Calif., 295 pp.

MILES, K. R., 1950. Garnetized Gabbros from the Eulaminna District, Mt. Margaret Gold field. *Bull. geol. Surv. W. Austral.* **103**, Pt. 2, 108–30.

MOREY, GEORGE W., 1957. The system water–nepheline–albite: a theoretical discussion. *Amer. J. Sci.* **255**, 461–80.

NORIN, ERIK, 1937. Reports from the Scientific Expedition to the northwestern provinces of China under leadership of Dr. Sven Hedin—The Sino-Swedish expedition—III. Geology; I, Geology of Western Qurug tagh, Eastern T'ien-shan. Stockholm: Thule. 195 pp.

OMORI, K., 1939. Optical properties of Japanese jade. *J. Jap. Ass. Mineralog.* **22**, 201–12 (in Japanese).

PABST, A., 1942. Re-examination of hibschite. *Amer. Min.* **27**, 783–92.

PALACHE, CHARLES, 1894. On a rock from the vicinity of Berkeley containing a new soda amphibole. *Bull. Univ. Calif. Dept. Geol. Sci.* **1**, 181–92.

PARK, C. F., 1946. The spilite and manganese problems of the Olympic Peninsula, Washington. *Amer. J. Sci.* **244**, 305–23.

PETTIJOHN, F. J., & BASTRON, H., 1959. Chemical composition of argillites of the Cobalt Series (Precambrian) and the problem of soda-rich sediments. *Bull. geol. Soc. Amer.* **70**, 593–600.

PHILLIPS, A. H., & HESS, H. H., 1936. Metamorphic differentiation at contacts between serpentine and siliceous country rocks. *Amer. Min.* **21**, 333–62.

PHILLIPS, R. M., 1939. The general geology of a part of San Benito County, California. Unpublished thesis for D.Ph. degree, Univ. of Calif., 76 pp.

PISTORIUS, C. W. F. T., & KENNEDY, G. C., 1960. Stability relations of grossularite and hydrogrossularite at high temperatures and pressures. *Amer. J. Sci.* **258**, 247–57.

RAMBERG, HANS, 1955. Natural and experimental boudinage and pinch-and-swell structures. *J. Geol.* **63**, 512–26.

READ, H. H., 1934. On zoned associations of antigorite, talc, actinolite, chlorite, and biotite in Unst, Shetland Islands. *Miner. Mag.* **23**, 519–40.

REED, J. J., 1957. Petrology of the Lower Mesozoic rocks of the Wellington District. *Bull. Geol. Surv. N.Z.* **57** (new series), 53 pp.

—— 1958. Regional metamorphism in southeast Nelson. Ibid. **58** (new series), 60 pp.

REED, R. D., 1951. Geology of California. *Am. Ass. Petrol. Geol.*, Tulsa, Oklahoma.

ROBERTSON, E. C., BIRCH, F., & MACDONALD, G. J. F., 1957. Experimental determination of jadeite stability relations to 25,000 bars. *Amer. J. Sci.* **255**, 115–37.

SAHA, P., 1959. Geochemical and X-ray investigation of natural and synthetic analcite. *Amer. Min.* **44**, 300–13.

SCHALLER, W. T., 1955. The pectolite–schizolite–serandite series. Ibid. **40**, 1022–31.

SCHÜLLER, K. H., 1958. Das Problem Akmit-Ägirin. *Heidelberg. Beitr. Min.* **6**, 112–38.

SEKI, Y., & SHIDO, F., 1959. Finding of jadeite from the Sanbagawa and Kamuikotan Metamorphic belts, Japan. *Proc. Japan Acad.* **35**, 137–8.

SHIDO, F., 1958. Calciferous amphibole rich in sodium from jadeite-bearing albitite of Kotaki, Niigata Prefecture. *J. geol. Soc. Japan*, **64**, 595–600.

—— & SEKI, YOTARO, 1959. Notes on rock-forming minerals. II. Jadeite and hornblende from the Kamuikotan metamorphic belt. *J. geol. Soc. Japan*, **65**, 673–7.

SMITH, J. R., & YODER, H. S., 1956. Variations in X-ray powder diffraction patterns of plagioclase feldspars. *Amer. Min.* **41**, 632–47.

SMITH, J. V., 1956. The powder patterns and lattice parameters of plagioclase feldspars. I. The soda-rich plagioclases. *Miner. Mag.* **31**, 47–68.


A

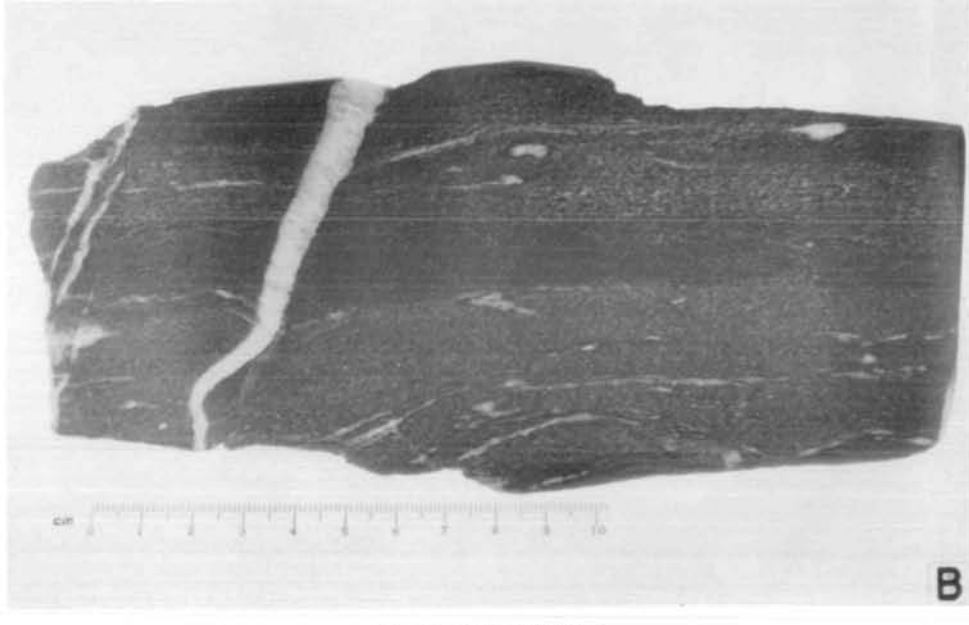
B

SUNDIUS, N., 1930. On the spilitic rocks. *Geol. Mag. Lond.* **67**, 1–17.
SWITZER, G., 1945. Eclogite from the California glaucophane schists. *Amer. J. Sci.* **243**, 1–8.
TALIAFERRO, N. L., 1943. Franciscan–Knoxville problem. *Bull. Amer. Ass. Petrol. Geol.* **27**, 109–219.
WARREN, B. E., & BISCOE, J., 1931. The crystal structure of the mono-clinic pyroxenes. *Z. Kristallogr.* **69**, 391–401.
WATSON, K. D., 1953. Prehnitization of albitite. *Amer. Min.* **38**, 197–206.
WOLFE, C. W., 1955. Crystallography of jadeite crystals from near Cloverdale, California. *Amer. Min.* **40**, 248–60.
YODER, H. S., 1950*a*. The jadeite problem: Parts I and II. *Amer. J. Sci.* **248**, 225–48, 312–34.
—— 1950*b*. Stability relations of grossularite. *J. Geol.* **58**, 221–53.
—— 1954. *Ann. Rep. geophys. Lab.*, Year Book No. **53**, 121–2.
—— 1955. Role of water in metamorphism. *Geol. Soc. Amer. Special Paper*, No. **62**, 505–24.
—— & CHESTERMAN, C. W., 1951. Jadeite of San Benito County, California. *Calif. Div. Mines Special Report*, **10**-C, 8 pp.
—— & TILLEY, C. E., 1959. *Ann. Rep. geophys. Lab.*, Year Book No. **58**, 90–91.
—— & WEIR, C. E., 1951. Change of free energy with pressure of the reaction nepheline+albite = 2 jadeite. *Amer. J. Sci.* **249**, 683–94.

EXPLANATION OF PLATE

FIG. A. Exposure of green jadeite–albite schist cut by white jadeite veins.

FIG. B. Polished slab of green jadeite–albite schist cut by veins of white jadeite. Original bedding planes are still preserved in the schist.